Anti-amnesic and neuroprotective effects of Fluoroethylnormemantine (FENM) in a pharmacological mouse model of Alzheimer's disease

Simon Couly, Morgane Denus, Mélanie Bouchet, Gilles Rubinstenn, Tangui Maurice

Anti-amnesic and neuroprotective effects of Fluoroethylnormemantine (FENM) in a pharmacological mouse model of Alzheimer's disease

Simon Couly, *PhD*, Morgane Denus, *MS*, Mélanie Bouchet, *MS*, Gilles Rubinstenn, *PhD*, Tangui Maurice, *PhD*

MMDN, Univ Montpellier, INSERM, EPHE, Montpellier, France (Drs Couly, Denus, Bouchet, Maurice); ReST Therapeutics, Paris, France (Dr Rubinstenn).

Running title: Neuroprotection by FENM in Aβ_{25-35}-injected mice

Regular research article

Word count of the body of the manuscript: 5292

Word count of the abstract: 251

Number of references: 60

Number of figures: 8

Number of tables: 3

Correspondence: Dr T. Maurice, INSERM UMR_S1198, Université de Montpellier, cc 105, Place Eugène Bataillon, 34095 Montpellier cedex 5, France. Tel.: +33/0 4 67 14 32 91. (tangui.maurice@umontpellier.fr),

Abstract

Background. Current therapies in Alzheimer's disease (AD), including Memantine, have proven to be only symptomatic but not curative nor disease-modifying. Fluoroethylnormemantine (FENM) is a structural analogue of Memantine, functionalized with a fluorine group that allowed its use as a positron emission tomography tracer. We here analyzed FENM neuroprotective potential in a pharmacological model of AD, in comparison to Memantine.

Methods: Swiss mice were treated intracerebroventricularly with aggregated $A\beta_{25-35}$ peptide and examined after one week in a battery of memory tests (spontaneous alternation; passive avoidance; object recognition; place learning in the water-maze; topographic memory in the Hamlet). Toxicity induced in the mouse hippocampus or cortex was analyzed biochemically or morphologically.

Results: Both Memantine and FENM showed symptomatic anti-amnesic effects in $A\beta_{25-35}$-treated mice. Interestingly, FENM was not amnesic when tested alone at 10 mg/kg, contrarily to Memantine. Drugs injected once-a-day prevented $A\beta_{25-35}$-induced memory deficits, oxidative stress (lipid peroxidation, cytochrome c release), inflammation (IL-6, TNFα increases; glial fibrillary acidic protein (GFAP) and Iba1 immunoreactivity in the hippocampus and cortex), and apoptosis and cell loss (Bax/Bcl-2 ratio; cell loss in the hippocampus CA1 area). However, FENM effects were more robust than observed with Memantine, with significant attenuations *vs.* the $A\beta_{25-35}$-treated group.

Conclusions: FENM therefore appeared as a potent neuroprotective drug in an AD model, with a superior efficacy as compared with Memantine, and an absence of direct amnesic effect at higher doses. These results open the possibility to use the compound at more relevant dosages than the ones actually proposed in Memantine treatment for AD.

Keywords: Fluoroethylnormemantine, Alzheimer's disease, symptomatic effect, neuroprotection, $A\beta_{25-35}$.

Introduction

Alzheimer's disease (AD) is characterized by the progressive deterioration of memory, cognition and autonomy (Bondi et al., 2017). AD is estimated to represent 60–80% of dementia cases and, at present, there are 50 million AD patients worldwide with its incidence doubling every 5 years after the age of 65 (Brookmeyer et al., 1998). The main clinical manifestations are a cognitive dysfunction, memory loss, and changes in personality. The pathology is characterized by the extracellular accumulation of aggregating amyloid-β (Aβ) proteins forming senile plaques, intracellular neurofibrillary tangles (NFTs), composed of abnormally phosphorylated tau protein, and a massive neuroinflammation (Selkoe, 1991, 2004; Bondi et al., 2017). Several hypotheses have been proposed to explain AD pathogenesis thereby involving amyloid cascade (Selkoe, 1991), tau hyperphosphorylation (Frost et al., 2009), neuroinflammation and oxidative stress (Butterfield & Halliwell, 2019). Toxicity results in synapse loss affecting cholinergic neurons innervating brain structures like the hippocampus or neocortex, and seems to be directly responsible for the memory impairments. Synapse loss results from the failure of neurons to maintain functional dendrites (Bloom, 2014; Avila et al., 2017) and is related to perturbed synaptic Ca^{2+} handling in response to over-activation of glutamate receptors, namely N-methyl-D-aspartate receptors (NMDARs) (Mota et al., 2014). Therefore, although the underlying causes and ideal strategy for a curative treatment remain elusive, present treatments are based on acetylcholinesterase inhibitors to maintain the cholinergic tonus, and on a NMDAR antagonist, Memantine (Danysz and Parsons, 2003; Wang and Reddy, 2017; Floch et al., 2018). Memantine is prescribed in moderate-to-severe AD and combining acetylcholinesterase inhibitors and Memantine led to higher benefits on cognitive alterations in patients (Patel and Grossberg, 2011; Deardorff and Grossberg, 2016). Memantine acts as a non-competitive NMDAR antagonist with moderate affinity, being an open NMDAR channel blocker with fast off-rate, but it also shows a preferential blockade of extrasynaptic NMDARs (Hardingham & Bading, 2010; Xia et al., 2010; Floch et al., 2018).

Present AD drugs provide only symptomatic benefits in patients (Salomone et al., 2012). In preclinical research models, Memantine, at 20 mg/kg/day, prevented quinolinic acid-induced lesion-induced learning impairments in rats in the T-maze and radial arm maze tests (Misztal et al., 1996; Zajaczkowski et al., 1996; Lang et al., 2004). Memantine, at 5 mg/kg/day, was also effective in rats against the $A\beta_{1-40}$ + ibotenic acid-induced memory deficits (Nakamura et al., 2006). Using intraventricularly injected lipopolysaccharide, a model of AD-like neuroinflammation, learning deficits in the water-maze test were prevented by Memantine, at 10 mg/kg, (Rosi et al., 2006). Finally, in mice receiving intraventricular injection of oligomerized $A\beta_{25-35}$, Memantine attenuated learning deficits at 1 mg/kg (Maurice, 2016). In transgenic mouse models of AD, Memantine at 30 mg/kg/day for 3 weeks improved acquisition in the water maze in APP/PS1 mice (Minkeviciene et al., 2004) and at 30 mg/kg for 12 weeks improved animals learning abilities and decreased memory loss in $APP_{Swe}/PS1^{dE9}$ mice fed with high-fat diet (Ettcheto et al., 2018). At 2 mg/kg daily, it alleviated retention deficits in the water-maze to the level of wildtype controls (Van Dam et al., 2005). Memantine is therefore neuroprotective in preclinical rodent models of AD. The reason why this effect does not translate in patients remains to be understood but it is worth noting that the proposed Memantine (Ebixa®) AD treatment is 20 mg/day, which corresponds to a lower dose than the ones used in preclinical neuroprotection studies. Recent results indicated that Memantine level in the cerebrospinal fluid during memantine treatment are not sufficient to trigger NMDA response (Valis et al., 2019).

Memantine and several derivatives have been fluorinated and tested as radiotracers of positron emission tomography (PET) for the *in vivo* labeling of NMDARs (Ametamey et al., 2002). Among them, [^{18}F]-Fluoromethylmemantine and [^{18}F]-Fluoroethylnormemantine ([^{18}F]-FENM) showed promising *in vitro* and *in vivo* binding in mice and monkeys, with good brain accumulation (Samnick et al., 1998; Ametamey et al., 1999; Salabert et al., 2015, 2018). [^{18}F]-Fluoromethylmemantine distribution did not however reflect regional NMDAR concentration, owing to high nonspecific uptake in white matter (Ametamey et al., 1999). Although having a moderate affinity (Ki = 3.5 10^{-6} M), the drug showed a good lipohily (logD = 1.93) and [^{18}F]-

FENM showed staining colocalization with NMDARs, with highest intensities found in the cortex and cerebellum and lowest in white matter (Salabert et al., 2015). A low non-specific binding was also observed when phencyclidine sites were blocked with (*R*,*S*)-ketamine (Salabert et al., 2015). As observed for Memantine, FENM is poorly metabolized *in vivo* with good stability in plasma and plasma protein binding, but with a low effective dosimetric dose as compared to other PET radiotracers (Salabert et al., 2018).

In the present study, we analyzed the symptomatic and neuroprotective activities of FENM, in comparison with Memantine, in the pharmacological model of AD induced by intraventricular injection of $A\beta_{25-35}$ peptide in mice (Maurice et al., 1996). After $A\beta_{25-35}$ injection, mice rapidly develop neuroinflammation, oxidative stress, apoptosis, and learning deficits reminiscent of AD toxicity (Meunier et al., 2006; Villard et al., 2011; Rodriguez Cruz et al., 2017; Maurice et al., 2019). Memantine and FENM were administered in the 0.1-10 mg/kg dose range either 7 days after $A\beta_{25-35}$ to examine the symptomatic effects of the drugs or o.d. during one week after the $A\beta_{25-35}$ injection to examine their neuroprotective effects (Meunier et al., 2006; Maurice et al., 2019). Learning deficits were analyzed using a battery of behavioral tests and neuroprotection was also examined in the hippocampus or cortex *post-mortem* using biochemical analyses of neuroinflammation, oxidative stress and apoptosis markers and using immunohistochemical and histological analyses of the mouse brains.

Material and methods

Animals

Male Swiss CD-1 (RjOrl:SWISS) mice or C57Bl/6j mice were from Janvier (Le Genest-Saint-Isle, France). All experiments were done with Swiss except the Hamlet test which used C57Bl/6j. Mice were aged 7-9 weeks, housed in groups of 8-10 mice, with free access to food and water, in a regulated environment (23 ± 1°C, 40-60% humidity, 12 h light/dark cycle. Animal procedures were conducted in adherence with the European Union Directive 2010/63 and the ARRIVE guidelines (Kilkenny et al., 2010) and authorized by the National Ethic Committee (Paris).

Drugs and peptides

3,5-Dimethyl-tricyclo[3.3.1.13,7]decyl amine (Memantine) was from Sigma-Aldrich (Saint-Quentin-Fallavier, France). 3(2-Fluoroethyl)tricyclo[3.3.1.13,7]decan-1-amine (Fluoroethylnormemantine, FENM) was from M2i Life Sciences (Saint-Cloud, France). Drugs were solubilized in physiological saline (NaCl 0.9%; vehicle solution) in a stock solution (2 mg/ml corresponding to the dose of 10 mg/kg) and dilutions done from this stock solution. The stock solutions were stored at +4°C up to two weeks. Drug were administered intraperitoneally (IP) in a volume of 100 µl per 20 g body weight.

The amyloid-β[25-35] peptide ($A\beta_{25-35}$) was from Eurogentec (Angers, France). It was solubilized in distilled water at 3 mg/ml and stored at -20°C until use. Before injection, the peptide was incubated at 37°C for 4 days, allowing oligomerization (Pike et al., 1993). Control injection was performed with vehicle solution (distilled water), as we previously described no effect of antisense or control peptide, and intracerebroventricularly (ICV) injections were done as described (Maurice et al., 1996).

Experimental series

We examined two effects of the drugs. First, symptomatic effects were analyzed in $A\beta_{25-35}$-treated mice by injecting the drugs just before the behavioral tests. Second, the neuroprotection was analyzed by repeatedly o.d. injecting the mice for one week starting on the day of peptide injection. For symptomatic effects, drugs were injected only on day 8 after $A\beta_{25-35}$ injection, 30 min before the behavioral tests: spontaneous alternation, passive avoidance training, session 2 of the object recognition test or each water-maze training sessions (Suppl. Fig. 1a). A group was tested for spontaneous alternation, passive avoidance and object recognition in series. As Memantine, and expectedly FENM, has a short half-life in mice (<2 h, Beconi et al., 2011), all the drug was excreted overnight. A separate group was trained in the Hamlet before $A\beta_{25-35}$ injection to assess topographic memory (Suppl. Fig. 1b). For neuroprotective effects, drugs were injected o.d. from day 1 to day 7 after $A\beta_{25-35}$ injection (Suppl. Fig. 1c) and mice were tested for spontaneous alternation, passive avoidance and object recognition in series. They were sacrificed at day 13 for immunochemistry (group A). A group of mice performed place learning in the water-maze, then sacrificed at day 16 and used for biochemical assays (group B). An additional series (group C) included mice sacrificed at day 5 after $A\beta_{25-35}$ peptide injection and daily drug injections for assessing cytokine levels by Elisa.

Behavioral testing

Procedures for each test are detailled in the Supplementary Material and followed our previously published work (Crouzier et al., 2018; Maurice et al., 1996, 2019; Meunier et al., 2006, 2013; Rodriguez Cruz et al., 2017; Villard et al., 2009, 2011). Spontaneous alternation in the Y-maze was used to assess spatial working memory. Long-term non-spatial memory was measured using a step-through passive avoidance test. Recognition memory was analyzed using a novel object test. Spatial reference memory was assessed using place learning in the water-maze. Topographic memory was assessed using the Hamlet test.

Lipid peroxidation measures

Mice from group B were sacrificed by decapitation 15 days after $A\beta_{25-35}$ injection and brains were rapidly removed, the hippocampus dissected out, weighed, frozen in liquid nitrogen and stored at -80°C until assayed. The level of lipid peroxidation was determined using the modified xylenol oxidation method as previously decribed (Meunier et al., 2006; Rodriguez Cruz et al., 2017).

Cytochrome c release

Mice were sacrificed at indicated days after injections and the hippocampus rapidly dissected on ice and kept at -80°C until used. For cytochrome c release experiments, the hippocampus were homogenized with a motorized homogenizer in ice-cold homogenization buffer (250 µM sucrose, 10 mM HEPES, pH 7.4), including a protease and phosphatase inhibitor cocktail (Roche Diagnostics, Meylan, France) in a final volume of 250 µl. Homogenates were centrifuged at 600 *g* for 5 min and the supernatant collected and centrifuged again at 10,300 *g* for 20 min. The supernatant, corresponding to the cytosolic fraction (C), and the pellet, corresponding to the crude mitochondrial fraction (M), were separated. The mitochondrial fraction was resuspended in 50 µl of ice-cold isolation buffer (250 mM mannitol, 5 mM HEPES, 0.5 mM EGTA, pH 7.4). Protein concentration was determined using a BCA assay (Pierce Biotechnology, Rockford, IL, USA) according to the manufacturer's instructions.

Proteins, 20 µg per lane, were resolved on a 12% SDS-polyacrylamid gel and transferred to a polyvinylidene fluoride (PVDF) membrane (GE Healthcare, Orsay, France). After 1 h blocking in 5% non-fat dry milk in a 20 mM Tris-buffered saline pH 7.5 buffer containing 0.1% Tween-20 (TBS-T), membranes were incubated overnight at 4°C with the following primary antibodies: mouse anti-cytochrome c (CytC, dilution 1/1000; BioLegend, San Diego, CA, USA), mouse anti-oxphos-complex IV subunit I (Oxphos, 1/1000; Invitrogen Life Technologies, St Aubin, France). After brief washes, membranes were incubated for 1 h at room temperature with corresponding secondary antibody: goat anti-mouse IgG peroxidase conjugate (1/2000; Sigma-Aldrich). The immunoreactive bands were visualized with the enhanced chemiluminescence reagent (ECL, Millipore, Molsheim, France) using an Odyssey®

Fc fluorescent imaging system (Li-Cor, Eurobio, Courtaboeuf, France). The intensity of peroxidase activity was quantified using the Odyssey® Fc software (Li-Cor).

Enzyme-linked immuno-sorbent assays (ELISA)

Protein contents in tumor necrosis factor-α (TNFα), interleukin-6 (IL-6), allograft inflammatory factor-1 (Iba-1), glial fibrillary acidic protein (GFAP), B-cell lymphoma 2 (Bcl-2) and Bcl-2–associated X (Bax) were analyzed by ELISA (see Table 1 for kit references). For n = 6-8 animals, both hippocampi were used. The tissue was homogenized after thawing in 1 ml of fresh lysis buffer (3 IS007, Cloud-Clone) and sonicated on ice for 2 x 10 s. After centrifugation (10,000 *g*, 5 min, 4°C), supernatants were then aliquoted and stocked at -80°C and used within a month for ELISA according to the manufacturer instructions. For each assay, absorbance was read at 450 nm and sample concentration was calculated using the standard curve. Results are expressed in ng of marker per mg of protein and in % of the control (V+V) value.

Brain fixation and slicing

At day 13, 5-6 mice from each condition of group A were anesthetized with 200 µl IP of a premix of ketamine (80 mg/kg) and xylazine (10 mg/kg) and transcardially perfused with 50 ml of saline solution followed by 50 ml of Antigenfix® (Diapath). The samples were kept for 48 h post-fixation in Antigenfix solution, at +4ºC. Brains were immersed in a sucrose 30% phosphate buffer saline (PBS) solution and sliced within a month.

Each brain was sliced in an area including the cortex, the nucleus basalis magnocellularis and the hippocampal formation, between Bregma +1.80 to -2.80 according to Paxinos & Franklin (2004). Serial coronal frozen sections (25 µm thickness) were cut with a freezing microtome (Microm HM 450, Thermo Fisher), collected in a 24 wells plate and stored in cryoprotectant at −20°C. Slices were then proceed on slides, each containing three coronal sections from one mouse.

Quantification of viable neurons in CA1 using Cresyl violet staining

Sections were stained with 0.2% Cresyl violet reagent (Sigma-Aldrich), then dehydrated with graded ethanol, treated with xylene, and mounted with Mountex medium (BDH Laboratory Supplies). After mounting, slides were kept drying at room temperature for 24 h. Examination of the CA1 area was performed using digitalized slices using a Nanozoomer virtual microscopy system (Hamamatsu, Massy, France). CA1 thickness measure and pyramidal cells count were processed using a 20 x objective with the cell count macro of ImageJ v1.46 software (NIH). Data were expressed as mean number of viable cells per mm^2, from 4-6 hippocampus for each mouse, according to the previously reported method (Villard et al., 2009; Rodriguez Cruz et al., 2017; Maurice et al., 2019).

Immunohistochemical labeling of microglia (Iba-1) and astrocytes (GFAP)

For immunohistochemical labeling slices in 24 wells plate were incubated overnight at +4°C with Rabbit polyclonal anti-Iba-1 (1:250, 019-19741, Wako) and mouse monoclonal anti-GFAP (1:400, G3893, Sigma-Aldrich). Then, slices were incubated 1 h at room temperature with secondary anti-rabbit Cy3 (1:1000) and secondary anti-mouse 488 (1:1000) antibodies. Slices were incubated 5 min with DAPI 10 ug/ml and rinsed with PBS. Finally, slices were mounted with ProLong (ThermoFischer). Pictures of each slices were taken with a confocal Microscope (Leica SPE).

Statistical analyses

Analyses were done using Prism v5.0 (GraphPad Software, San Diego, CA, USA). Data were analyzed using one-way analyses of variance (ANOVA, *F* value), followed by a Dunnett's test. Passive avoidance latencies, expressed as median and interquartile range and represented as box-and-whiskers, were analyzed using a nonparametric Kruskal-Wallis ANOVA (*H* value) and *post-hoc* comparisons done using a Dunn's test. Probe test data in the water-maze were presented as time spent in the T and o quadrants or object preferences, calculated from the number or duration of contacts with the two objects, were analyzed using a one-sample *t*-test

vs. the chance level (15 s or 50%). Significance levels were $p < 0.05$, $p < 0.01$ and $p < 0.001$. Statistical data are indicated in the figure legends.

Results

Anti-amnesic effects of Memantine and FENM in $A\beta_{25-35}$-injected mice

We first analyzed the symptomatic effects of FENM, in comparison with Memantine, on $A\beta_{25-35}$-induced learning deficits in mice. Drugs were injected 30 min before the tests, particularly before the training session(s) in long-term memory tests, and 7 days after $A\beta_{25-35}$ injection (Suppl. Fig. 1a). Memantine dose-dependently attenuated $A\beta_{25-35}$-induced spontaneous alternation deficits in mice, in a bell-shaped manner (Fig. 1a), with a significant effect at 0.3 mg/kg. FENM showed a similar dose-response effect (Fig. 1b) and significant attenuation was observed in the 0.3-10 mg/kg dose range. In the passive avoidance test, Memantine dose-dependently attenuated $A\beta_{25-35}$-induced deficit in a bell-shaped manner with a significant effect at 0.3 mg/kg (Fig. 1c). FENM showed a similar dose-response effect with significance in the 0.1-1 mg/kg dose range (Fig. 1d). In the object recognition test, drugs were injected before session 2. Drugs did not affect the equal exploration of the 2 similar objects (Figs. 1e, 1f). In session 3, Memantine and FENM attenuated significantly but in a bell-shaped manner the $A\beta_{25-35}$-induced novel object exploration deficit, at doses of 0.3 mg/kg and higher (Figs. 1g, 1h).

In the water-maze test, $A\beta_{25-35}$ injection resulted in a moderate attenuation of the decrease in swimming latency to find the platform as compared to Veh-treated animals during trials 4 and 5 (Fig. 2a), indicating that $A\beta_{25-35}$ fails to affect procedural memory but rather impaired integration of spatial cues that contributed the mouse efficiency to locate the platform in late training sessions. $A\beta_{25-35}$ injection resulted in memory deficits since the time spent in the T quadrant during the probe test was at the random level (15 s) contrarily to control animals (Fig. 2c). FENM, tested at the most active dose identified previously, 0.3 mg/kg, restored an acquisition profile similar to controls (Fig. 2b) and a significantly increased exploration of the T quadrant during the probe test (Fig. 2c).

The drug symptomatic effect was finally tested in an alert sign of Alzheimer's disease, the spatio-temporal disorientation, as it could be analyzed in the Hamlet test (Crouzier et al., 2018). Mice were trained in the Hamlet for 4 h/day for 2 weeks (Suppl. Fig. 1b) and identified

the maze topography (localization of the Run, Drink, Eat, Hide and Interact houses) by latent learning during exploration. When tested in a water-deprived (WD) condition, they did less errors (Fig. 2d) and spent less time (Fig. 2g) to reach the Drink house as compared when tested in a non-water-deprived (NWD) condition. They were injected with $A\beta_{25-35}$ peptide 2 h after the probe test and retested after 1 week. The non-treated mice still showed a lower number of errors and lower latency to reach the goal house in WD condition, but not $A\beta_{25-35}$-treated mice (Fig. 2e, 2h). Interestingly, while Memantine treated $A\beta_{25-35}$ mice failed to show a difference between NWD and WD conditions, FENM significantly restored an effective topographic memory (Figs. 2e, 2h). Calculations of the disorientation index, as proposed by Crouzier et al. (2018) using either the errors or latencies (Figs. 2f, 2i), confirmed that $A\beta_{25-35}$ induced a significant spatio-temporal disorientation that was completely prevented by FENM, while Memantine had no or little effects on topographic memory impairments in $A\beta_{25-35}$-injected mice (Figs. 2f, 2i).

These data showed that both Memantine and FENM, at sub-mg/kg doses, *i.e.*, a dose level equivalent to the one proposed in human for AD, attenuated $A\beta_{25-35}$-induced learning deficits in numerous forms of memories. As Memantine, but not FENM, showed at the highest dose tested 10 mg/kg rather a worsening of memory abilities in the Y-maze and passive avoidance tests (Fig. 1c), drugs were also tested alone in control mice. As shown in Table 2, Memantine, but not FENM, impaired learning in both tests at 10 mg/kg, suggesting some difference in the modes of action of Memantine and FENM on NMDARs.

3.2. Protective effects of Memantine and FENM in $A\beta_{25-35}$-injected mice

We analyzed the protective potential of FENM, in comparison with Memantine, against $A\beta_{25-35}$-induced memory deficits and toxicity in mice. Drugs were injected o.d. between day 1 and 7 after $A\beta_{25-35}$ and mice were tested behaviorally without further drug injection (Suppl. Fig. 1c). Memantine and FENM prevented $A\beta_{25-35}$-induced spontaneous alternation deficits in mice (Figs. 3a, 3b), at doses of 0.1-3 mg/kg. The drugs also prevented $A\beta_{25-35}$-induced passive avoidance deficit in the same dose range, but with significance reached at the doses of 0.1

and 1 mg/kg only for Memantine (Fig. 3c) contrarily to FENM, active at all 0.1-3 mg/kg doses (Fig. 3d). In the object recognition test, treatments did not affect the equal exploration of the 2 similar objects (Figs. 3e, 3f). However, Memantine and FENM prevented $A\beta_{25-35}$-induced object recognition deficit in the same dose range, but with significance reached at the doses of 0.1 and 1 mg/kg only for Memantine (Fig. 3g) contrarily to FENM, active at all 0.1-3 mg/kg doses (Fig. 3h). In the water-maze test, the drugs at 0.3 mg/kg restored an acquisition profile similar to controls (Fig. 4a, 4b) but only FENM restored a significant exploration of the T quadrant during the probe test (Fig. 4c). These observations showed at on the behavioral level, Memantine and FENM protected against $A\beta_{25-35}$-induced memory impairments in mice.

Several biochemical parameters of $A\beta_{25-35}$-induced toxicity were analyzed in the mouse hippocampus or cortex. First, alteration of mitochondrial function was measured by the level of cytochrome c released into the cytosol. Cytosolic and mitochondrial fractions were isolated, and the latter identified using Oxphos immunoreactivity (Fig. 5a). $A\beta_{25-35}$ induced a significant increase in cytochrome c release, measured as cytosol/mitochondria content ratio, that was attenuated by Memantine and FENM (Fig. 5b). A consequence of mitochondrial alteration is an increased oxidative stress and resulting peroxidation of membrane lipids. $A\beta_{25-35}$ induced a +47% increase in lipid peroxidation that was attenuated by Memantine and significantly prevented by FENM (Fig. 5c).

Several markers of neuroinflammation were analyzed In hippocampus extracts. The levels of cellular markers of reactive microglia (Iba-1) or reactive astrocytes (GFAP) were moderately increased 2 weeks after $A\beta_{25-35}$ (Figs. 5d, 5e). However, at a shorter delay of 5 days after $A\beta_{25-35}$, cytokines contents were markedly increased: +83% for IL-6 (Fig. 5f) and +57% for TNFα (Fig. 5g). Memantine attenuated while FENM fully prevented the increases in these cytokines (Figs. 5f, 5g).

The treatments failed to significantly affect the levels of the anti-apoptotic protein Bcl-2, with just a trend to increased level in all $A\beta_{25-35}$ groups (Fig. 5h). However, $A\beta_{25-35}$ increased the content in pro-apoptotic protein Bax by +54% (Fig. 5i). Memantine and FENM significantly

prevented this increase. Consequently, the Bax/Bcl-2 ratio was slightly increased by $A\beta_{25-35}$ and this increase was prevented by the drugs but only significantly by FENM (Fig. 5j).

Apoptosis results in cell death, particularly in a very sensitive area like the pyramidal cell layer of the hippocampus. $A\beta_{25-35}$ injection resulted in a significant -13% decrease in viable cells stained with cresyl violet (Figs. 6a, 6b, 6e) and in a +12% increase in the layer thickness, as toxicity resulted in cell swelling (Figs. 6a, 6b, 6f). Memantine and FENM prevented these alterations, both in terms of viable cells (Figs. 6c, 6d, 6e) and layer thickness (Figs. 6c, 6d, 6f).

Since global tissue analysis of neuroinflammatory markers by Elisa failed to show an effect of the peptide injection, neuroinflammation was also analyzed using immunohistochemistry and several brain regions were analyzed: the stratum radiatum (Rad), molecular (Mol) and polymorph layers of the dentate gyrus (PoDG) in the hippocampus and the lateral parietal associative cortex (Fig. 6g). GFAP immunolabelling in the hippocampal subfields showed an intense astroglial reaction, and cell counting showed significant increases in the Rad (Figs. 7a-e) and Mol (Figs. 7f-j) and a trend in PoDG (Figs. 7k-o). Memantine attenuated GFAP immunolabelling in the Rad and PoDG but not Mol, while FENM showed significant prevention of $A\beta_{25-35}$-induced increases in all 3 structures (Figs. 7e, 7j, 7o). Iba-1 immunolabelling was increased significantly in Rad (Figs. 8a-e), showed only a marked trend in Mol (Figs. 8f-j) and no change in PoDG (Figs. 8k-o). Both treatments decreased $A\beta_{25-35}$-induced increases in Iba-1 labelling in Rad (Fig. 8e) and showed significant decreases even as compared to the Sc.Aβ group level in PoDG (Fig. 8o). In the cortex, $A\beta_{25-35}$ induced significant increases in GFAP (Suppl. Figs. 2a-e) and Iba-1 labelling (Suppl. Figs. 2f-j). Memantine failed to prevent $A\beta_{25-35}$-induced increases contrarily to FENM that showed significantly effects (Suppl. Figs. 2e, 2j).

These data show that both Memantine and FENM are protective against $A\beta_{25-35}$-induced behavioral deficits, neuroinflammation, oxidative stress, apoptosis, and cell loss, with FENM showing a more marked prevention on neuroinflammation, oxidative stress, and apoptosis parameters measured than Memantine.

Discussion

We used the pharmacological mouse model of AD induced by ICV injection of oligomeric $A\beta_{25-35}$ peptide to analyze the symptomatic and neuroprotective effects of FENM and its parent molecule Memantine. $A\beta_{25-35}$ induced a rapid toxicity, with oxidative stress and mitochondrial alteration (Meunier et al., 2006; Lahmy et al., 2015), neuroinflammation (Rodriguez Cruz et al., 2017), apoptosis, synapse and cell loss (Maurice et al., 2013; Chumakov et al., 2015), and learning impairments (Maurice et al., 1996, 2019; Meunier et al., 2006; Lahmy et al., 2015). Moreover, $A\beta_{25-35}$ injection also activated the kinases, GSK-3β, Cdk5 and MAPK, responsible for abnormal tau phosphorylation (Klementiev et al., 2007; Lahmy et al., 2013) and the secretases responsible for $A\beta_{1-42}$ protein generation (Klementiev et al., 2007; Meunier et al., 2013). Although no evidence demonstrated that tau hyperphosphorylation and increased $A\beta_{1-42}$ protein effectively contributed to the toxicity observed in the $A\beta_{25-35}$ model, the pattern of toxicity appears highly coherent with AD neurotoxicity and the model represents a coherent acute model of AD-like pathology. It allows the rapid and pertinent screening of symptomatic or neuroprotective drugs that will likely show efficacy after chronic treatment in transgenic mouse models of AD. For instance, a low sialic acid form of erythropoietin injected intranasally was found active in the $A\beta_{25-35}$ model (Maurice et al., 2013) and in $hAPP_{Swe}$ mice after a 2-month chronic treatment (Rodriguez Cruz et al., 2017), and a combined therapy with baclofen and acamprosate was found as active in $A\beta_{25-35}$ mice as in $hAPP_{Swe,Lon}$ mice (Chumakov et al., 2015). The $A\beta_{25-35}$ model is therefore a suitable model to explore the therapeutic potentiality of new drugs and to compare it with clinical reference drugs, such as Memantine.

We first observed that FENM and Memantine, when injected 30 min before the behavioral tests, reversed the $A\beta_{25-35}$-induced learning impairments. As summarized in Table 3a, Memantine and FENM were effective at doses around 0.3 mg/kg in the different tests. Memantine was effective in the 0.3-3 mg/kg dose-range in the spontaneous alternation, passive avoidance and object recognition tests. The drug is active at 0.3 mg/kg in the water-maze test (Table 3a). FENM also showed efficacy in the 0.1-1 mg/kg dose-range in the

spontaneous alternation test, with a dose-response profile comparable to MEM. FENM was particularly effective in the object recognition test. The compound was also effective in the water-maze, at 0.3 mg/kg. The observation that all types of memory were restored by FENM or Memantine confirmed the efficacy of the drugs to restore a functional glutamatergic neurotransmission and glutamatergic/cholinergic dialog in the hippocampus and cortex, as these neurotransmitters sustain learning processes in these different tests (Aigner, 1995). Interestingly, we observed that FENM was more effective than Memantine to restore complex memory. Indeed, the disorientation index in the Hamlet test, which measures spatial orientation and relies on both allocentric and egocentric strategies (Crouzier et al., 2018), returned to zero after FENM but not Memantine. At the tested dose of 0.3 mg/kg, FENM therefore appeared more effective on this alert sign of AD.

The drugs were then examined for their protective potency against $A\beta_{25-35}$-induced toxicity. They were administered o.d. and mice were then examined for their behavioral responses without further drug administration. Memantine was protective against $A\beta_{25-35}$-induced learning impairments in the 0.1-3 mg/kg dose-range, in the spontaneous alternation, passive avoidance and object recognition tests (Table 3b). The dose of 0.3 mg/kg attenuated $A\beta_{25-35}$-induced place learning deficits in the water-maze but in a non-significant manner. FENM was also protective in the 0.1-3 mg/kg dose-range against $A\beta_{25-35}$-induced learning impairments, in all three tests. Furthermore, the dose of 0.3 mg/kg attenuated $A\beta_{25-35}$-induced learning deficits in the water-maze in a significant manner (Table 3b). Biochemical analyses of several markers were performed on tissue extracts. Analyses of the levels of cytochrome c release into the cytosol and of lipid peroxidation in the cortical tissue showed that Memantine non-significantly attenuated while FENM completely prevented $A\beta_{25-35}$-induced oxidative stress partly due to mitochondrial dysfunction (Table 3b). Bax levels were highly significantly increased by the $A\beta_{25-35}$ injection and this increase was significantly prevented by both Memantine and FENM. Results expressed as Bax/Bcl-2 ratios confirmed the drug efficacies but only FENM significantly decreased the $A\beta_{25-35}$-induced increase in Bax/Bcl-2 ratio. The levels of IL-6 and TNFα measured at a short delay (5 days) after $A\beta_{25-35}$ showed that

Memantine non-significantly attenuated while FENM completely prevented $A\beta_{25-35}$-induced inflammation. A precise immunofluorescence analysis of neuroinflammation was performed in several glial reacting areas of the hippocampus (Rad, Mol, PoDG), as previously described (Villard et al., 2009; Maurice et al., 2019) and in one cortical area taken in the same coronal plane (LPtA). Both astroglial and microglial reactions were observed in the Rad and Mol areas, while the change appeared limited in PoDG. Memantine significantly attenuated astroglial reaction in Rad, but not in Mol. FENM attenuated it in both areas (Table 3b). Both drugs attenuated microglial reactions in these areas, but only FENM led to a significant difference, in the Rad. In the cortex, $A\beta_{25-35}$-induced significant increases in both GFAP and Iba-1 expressed cells. Memantine marginally affected this increase while it was significantly prevented by FENM (Table 3b). FENM therefore appeared to result in a greater anti-inflammatory effect than Memantine. Neuronal cell loss was estimated in the CA1 pyramidal cell layer of the hippocampus, using a viable cell staining with Cresyl violet (Villard et al., 2009; Maurice et al., 2019). The number of cells was significantly decreased by 13% after $A\beta_{25-35}$ injection and the remaining cells markedly swelled thus increasing the layer thickness by 12%. Both Memantine and FENM significantly prevented cell loss and layer thickening.

These observations confirmed previous data showing that Memantine is neuroprotective in preclinical rodent models of AD. This was observed in the $A\beta_{25-35}$ model, the drug attenuating learning impairments, changes in neuropeptides, enzymes, glial markers and iNOS activity induced by the peptide (Arif & Kato, 2009; Arif et al., 2009; Maurice, 2016). Wang et al. (2015) reported that in a rat model of AD induced by intracerebroventricular injection of an adeno-associated viral vector overexpressing the protein phosphatase-2A (PP2A) inhibitor, Memantine, at 2 mg/kg orally daily during 6 weeks, rescued PP2A activity, attenuated AD-like pathology and cognitive deficits in the rats. In transgenic models, the drug showed symptomatic and neuroprotective effects in the $hAPP_{Swe}$, APP/PS1, APP23, and 3xTg-AD lines (Minkevicienne et al., 2004; Van Dam et al., 2005; Van Dam & De Deyn, 2006; Dong et al., 2008). So, contraily to its use in clinic resulting in limited symptomatic effects, Memantine coherently led to symptomatic and neuroprotective effect in preclinical models.

The biochemical and morphological analyses showed that the novel derivative FENM induced a more clear-cut neuroprotection, particularly on oxidative stress and apoptosis markers and on neuroinflammation markers in the hippocampus and cortex. The drug acts as its parent molecule, as a weak non-competitive NMDAR antagonist. Although the precise mode of action of FENM needs to be further refined using adequate electrophysiological analyses, the drug labeled NMDARs in the brain when used as a PET radiotracer (Salabert et al., 2015, 2018). The mechanism of action of Memantine was also found to involve several cellular regulation pathways, beyond its effect at NMDARs. The drug protected against Aβ oligomers-induced reactive oxygen species formation (De Felice et al., 2007), stimulated cholinergic signaling through muscarinic acetylcholine receptors (Drever et al., 2007), regulated nerve growth factor (NGF) signaling by increasing TrkA activation and decreasing p75NTR signaling (Liu et al., 2014), and regulated protein phosphatase-2A activation (Wang et al., 2015). FENM likely shares these different effects in AD mice, but the drug appeared more effective in preventing oxidative stress and neuroinflammation and failed to induced learning deficits at a high dose (10 mg/kg). FENM may therefore present additional targets or a slightly different mechanism of action NMDARs that deserve to be analyzed.

FENM appeared as a promising drug. It effect must now be confirmed in transgenic mouse models of AD. Only repeated administration regimen in these chronic models will allow to determine if FENM is able to decrease amyloid load and plaque formation in amyloid-based models or kinases activities and neurofibrillary tangles formation in tau-based models. This was previously described for Memantine (Wang et al., 2015) and several other drugs with similar symptomatic and neuroprotective profiles. The strength of FENM-induced neuroprotection must be investigated in similar transgenic models in the future, in parallel to the anlaysis of the drug mechanism of action, in order to establish the superiority of the molecule over Memantine and to determine whether the drug is a putative candidate for synergic combinations with current drugs under development.

In conclusion, we described the symptomatic and neuroprotective efficacy of a novel Memantine derivative, FENM, in a pharmacological mouse model of AD. Comparison with its

parent molecule revealed that FENM is more effective in preventing oxidative stress, apoptosis and neuroinflammation and suggested that the molecule may not only be used as a potent PET radiotracer for NMDAR, but also as a promising neuroprotective drug in AD. Moreover, the compound may be used at more relevant dosages than the ones actually proposed with the Memantine treatment.

Acknowledgements

The authors thank Marc Criton and Lorène Milliex (SATT AxLR, Montpellier, France) for regular advices during the project; Dr Christine Denny (University of Columbia, NY, USA) for careful reading of the manuscript; M2i Life Sciences for providing FENM; and the CECEMA animal facility of the University of Montpellier.

T. Maurice designed the study; S. Couly and G. Rubinstenn amended the study design; S. Couly, M. Denus and M. Bouchet performed the behavioral, immunohistochemical, and biochemical analyses; S. Couly and T. Maurice analyzed the data. T. Maurice wrote the draft version of the manuscript; S. Couly and G. Rubinstenn corrected the manuscript. All authors approved the final version.

This work was supported by a grant from SATT AxLR (FR-2005-138) to T. Maurice.

Declaration of Competing Interest

G. Rubinstenn is co-inventor and owner of the patent FR-2005-138 pending and is founder of ReST Therapeutics. T. Maurice is co-inventor of the patent FR-2005-138 pending. Other authors declare no conflict of interest.

Significance statement

Currently available therapeutic strategies in Alzheimer's disease show limited efficacy, particularly in terms of long lasting neuroprotection and potential disease-modifying action. Among clinical drugs, Memantine is a non-competitive NMDA receptor antagonist with marked anti-hypoxic and synapse stabilizing effects. We here described a memantine derivative, Fluoroethylnormemantine (FENM) with superior pharmacological efficacy than its parent molecule. The drug showed potent symptomatic and neuroprotective effects in a pharmacological mouse model of Alzheimer's disease with no amnesic effect by itself at high dose. The drug, already used as a PET radiotracer, deserves to be further developed as a novel neuroprotective agent.

References

Aigner TG (1995) Pharmacology of memory: cholinergic-glutamatergic interactions. Curr Opin Neurobiol. 5:155-60.

Ametamey SM, Bruehlmeier M, Kneifel S, Kokic M, Honer M, Arigoni M, Buck A, Burger C, Samnick S, Quack G, Schubiger PA (2002) PET studies of 18F-memantine in healthy volunteers. Nucl Med Biol 29:227–31.

Ametamey SM, Samnick S, Leenders KL, Vontobel P, Quack G, Parsons CG, Schubiger PA (1999) Fluorine-18 radiolabelling, biodistribution studies and preliminary PET evaluation of a new memantine derivative for imaging the NMDA receptor. J Recept Signal Transduct Res 19:129–41.

Arif M, Chikuma T, Ahmed MM, Nakazato M, Smith MA, Kato T (2009) Effects of memantine on soluble $A\beta_{25-35}$-induced changes in peptidergic and glial cells in Alzheimer's disease model rat brain regions. Neuroscience. 164:1199-209.

Arif M, Kato T (2009) Increased expression of PAD2 after repeated intracerebroventricular infusions of soluble $A\beta_{25-35}$ in the Alzheimer's disease model rat brain: effect of memantine. Cell Mol Biol Lett. 14:703-14.

Avila J, Llorens-Martín M, Pallas-Bazarra N, Bolós M, Perea JR, Rodríguez-Matellán A, Hernández F (2017) Cognitive Decline in Neuronal Aging and Alzheimer's Disease: Role of NMDA Receptors and Associated Proteins. Front Neurosci. 11:626.

Beconi MG, Howland D, Park L, Lyons K, Giuliano J, Dominguez C, Munoz-Sanjuan I, Pacifici R (2011) Pharmacokinetics of memantine in rats and mice. Version 2. PLoS Curr. 3:RRN1291.

Bloom GS (2014) Amyloid-β and tau: the trigger and bullet in Alzheimer disease pathogenesis. JAMA Neurol. 71:505-8.

Bondi MW, Edmonds EC, Salmon DP (2017) Alzheimer's disease: past, present, and future. J Int Neuropsychol Soc. 23:818–31.

Brookmeyer R, Gray S, Kawas C (1998) Projections of Alzheimer's disease in the United States and the public health impact of delaying disease onset. Am J Public Health. 88:1337–42.

Butterfield DA, Halliwell B; (2019) Oxidative stress, dysfunctional glucose metabolism and Alzheimer disease. Nat Rev Neurosci. 20:148–60.

Chumakov I, Nabirotchkin S, Cholet N, Milet A, Boucard A, Toulorge D, Pereira Y, Graudens E, Traoré S, Foucquier J, Guedj M, Vial E, Callizot N, Steinschneider R, Maurice T, Bertrand V, Scart-Grès C, Hajj R, Cohen D (2015) Combining two repurposed drugs as a promising approach for Alzheimer's disease therapy. Sci Rep. 5:7608.

Crouzier L, Gilabert D, Rossel M, Trousse F, Maurice T (2018) Topographical memory analyzed in mice using the Hamlet Test, a novel complex maze. Neurobiol Learn Mem. 149:118-134.

Crouzier L, Maurice T (2018) Assessment of topographic memory in mice in a complex environment using the Hamlet test. Current Protoc Mouse Biol. 8:e43.

Danysz W, Parsons CG (2003) The NMDA receptor antagonist memantine as a symptomatological and neuroprotective treatment for Alzheimer's disease: preclinical evidence. Int J Geriatr Psychiatry. 18:S23-32.

De Felice FG, Velasco PT, Lambert MP, Viola K, Fernandez SJ, Ferreira ST, Klein WL (2007) Aβ oligomers induce neuronal oxidative stress through an N-methyl-D-aspartate receptor-dependent mechanism that is blocked by the Alzheimer drug memantine. J Biol Chem. 282:11590-601.

Deardorff WJ, Grossberg GT (2016) Pharmacotherapeutic strategies in the treatment of severe Alzheimer's disease. Expert Opin Pharmacother. 17:1789-800.

Dong H, Yuede CM, Coughlan C, Lewis B, Csernansky JG (2008) Effects of memantine on neuronal structure and conditioned fear in the Tg2576 mouse model of Alzheimer's disease. Neuropsychopharmacology. 33:3226-36.

Drever BD, Anderson WG, Johnson H, O'Callaghan M, Seo S, Choi DY, Riedel G, Platt B (2007) Memantine acts as a cholinergic stimulant in the mouse hippocampus. J Alzheimers Dis. 12:319-33.

Ettcheto M, Sánchez-López E, Gómez-Mínguez Y, Cabrera H, Busquets O, Beas-Zarate C, García ML, Carro E, Casadesus G, Auladell C, Vázquez Carrera M, Folch J, Camins A. Peripheral and central effects of memantine in a mixed preclinical mice model of obesity and familial Alzheimer's disease. Mol Neurobiol. 2018;55:7327-39.

Folch J, Busquets O, Ettcheto M, Sánchez-López E, Castro-Torres RD, Verdaguer E, Garcia ML, Olloquequi J, Casadesús G, Beas-Zarate C, Pelegri C, Vilaplana J, Auladell C, Camins A. Memantine for the treatment of dementia: a review on its current and future applications. J Alzheimers Dis. 2018;6:1223-40.

Frost B, Jacks RL, Diamond MI (2009) Propagation of tau misfolding from the outside to the inside of a cell. J Biol Chem. 284:12845–52.

Hardingham GE, Bading H (2010) Synaptic versus extrasynaptic NMDA receptor signalling: implications for neurodegenerative disorders. Nat Rev Neurosci. 11:682-96.

Kilkenny C, Browne W, Cuthill IC, Emerson M, Altman DG; NC3Rs Reporting Guidelines Working Group (2010) Animal research: reporting in vivo experiments: the ARRIVE guidelines. Br J Pharmacol. 160:1577-9.

Klementiev B, Novikova T, Novitskaya V, Walmod PS, Dmytriyeva O, Pakkenberg B, Berezin V, Bock E (2007) A neural cell adhesion moleculederived peptide reduces neuropathological signs and cognitive impairment induced by $A\beta_{25–35}$. Neuroscience 145:209–224.

Lahmy V, Long R, Morin D, Villard V, Maurice T (2015) Mitochondrial protection by the mixed muscarinic/σ1 ligand ANAVEX2-73, a tetrahydrofuran derivative, in $A\beta_{25-35}$ peptide-injected mice, a nontransgenic Alzheimer's disease model. Front Cell Neurosci. 8:463.

Lahmy V, Meunier J, Malmström S, Naert G, Givalois L, Kim SH, Villard V, Vamvakides A, Maurice T (2013) Blockade of Tau hyperphosphorylation and $A\beta_{1-42}$ generation by the aminotetrahydrofuran derivative ANAVEX2-73, a mixed muscarinic and σ_1 receptor

agonist, in a nontransgenic mouse model of Alzheimer's disease. Neuropsychopharmacology. 38:1706-23.

Lang UE, Mühlbacher M, Hesselink MB, Zajaczkowski W, Danysz W, Danker-Hopfe H, Hellweg R (2004) No nerve growth factor response to treatment with memantine in adult rats. J Neural Transm. 111:181-90.

Liu MY, Wang S, Yao WF, Zhang ZJ, Zhong X, Sha L, He M, Zheng ZH, Wei MJ (2014) Memantine improves spatial learning and memory impairments by regulating NGF signaling in APP/PS1 transgenic mice. Neuroscience. 2273:141-51.

Maurice T (2016) Protection by sigma-1 receptor agonists is synergic with donepezil, but not with memantine, in a mouse model of amyloid-induced memory impairments. Behav Brain Res. 296:270-278.

Maurice T, Lockhart BP, Privat A (1996) Amnesia induced in mice by centrally administered β-amyloid peptides involves cholinergic dysfunction. Brain Res. 706:181-93.

Maurice T, Mustafa MH, Desrumaux C, Keller E, Naert G, de la C. García-Barceló M, Rodríguez Cruz Y, Garcia Rodríguez JC (2013). Intranasal formulation of erythropoietin EPO) showed potent protective activity against amyloid toxicity in the $A\beta_{25-35}$ nontransgenic mouse model of Alzheimer's disease. J Psychopharmacol. 27;1044-57.

Maurice T, Volle JN, Strehaiano M, Crouzier L, Pereira C, Kaloyanov N, Virieux D, Pirat JL (2019) Neuroprotection in non-transgenic and transgenic mouse models of Alzheimer's disease by positive modulation of σ_1 receptors. Pharmacol Res. 144:315-330.

Meunier J, Ieni J, Maurice T (2006) The anti-amnesic and neuroprotective effects of donepezil against amyloid β_{25-35} peptide-induced toxicity in mice involve an interaction with the σ_1 receptor. Br J Pharmacol. 149: 998-1012.

Meunier J, Villard V, Givalois L, Maurice T (2013) The γ-secretase inhibitor 2-[(1R)-1-[(4-chlorophenyl)sulfonyl] (2,5-difluorophenyl)amino]ethyl-5-fluorobenzenebutanoic acid (BMS-299897) alleviates $A\beta_{1-42}$ seeding and short-term memory deficits in the $A\beta_{25-35}$ mouse model of Alzheimer's disease. Eur J Pharmacol. 698:193-9.

Minkeviciene R, Banerjee P, Tanila H (2004) Memantine improves spatial learning in a transgenic mouse model of Alzheimer's disease. J Pharmacol Exp Ther. 311:677-82.

Misztal M, Frankiewicz T, Parsons CG, Danysz W (1996) Learning deficits induced by chronic intraventricular infusion of quinolinic acid--protection by MK-801 and memantine. Eur J Pharmacol. 296:1-8.

Mota SI, Ferreira IL, Rego AC (2014) Dysfunctional synapse in Alzheimer's disease - A focus on NMDA receptors. Neuropharmacology. 76:16-26.

Nakamura S, Murayama N, Noshita T, Katsuragi R, Ohno T (2006) Cognitive dysfunction induced by sequential injection of amyloid-beta and ibotenate into the bilateral hippocampus; protection by memantine and MK-801. Eur J Pharmacol. 548:115-22.

Patel L, Grossberg GT (2011) Combination therapy for Alzheimer's disease. Drugs Aging. 28:539-46.

Paxinos G, Franklin KBJ (2004) The Mouse Brain in Stereotaxic Coordinates. Academic Press, San Diego, CA, USA.

Pike CJ, Burdick D, Walencewicz AJ, Glabe CG, Cotman CW (1993) Neurodegeneration induced by beta-amyloid peptides in vitro: the role of peptide assembly state. J Neurosci. 13:1676-87.

Rodríguez Cruz Y, Strehaiano M, Rodríguez Obaya T, García Rodríguez JC, Maurice T (2017) An intranasal formulation of erythropoietin (Neuro-EPO) prevents memory deficits and amyloid toxicity in the APPSwe transgenic mouse model of Alzheimer's disease. J Alz Dis. 55:231-248.

Rosi S, Vazdarjanova A, Ramirez-Amaya V, Worley PF, Barnes CA, Wenk GL (2006) Memantine protects against LPS-induced neuroinflammation, restores behaviorally-induced gene expression and spatial learning in the rat. Neuroscience. 142:1303-15.

Salabert AS, Fonta C, Fontan C, Adel D, Alonso M, Pestourie C, Belhadj-Tahar H, Tafani M, Payoux P (2015) Radiolabeling of [^{18}F]-fluoroethylnormemantine and initial in vivo evaluation of this innovative PET tracer for imaging the PCP sites of NMDA receptors. Nucl Med Biol. 42:643-53.

Salabert AS, Mora-Ramirez E, Beaurain M, Alonso M, Fontan C, Tahar HB, Boizeau ML, Tafani M, Bardiès M, Payoux P (2018) Evaluation of [^{18}F]FNM biodistribution and dosimetry based on whole-body PET imaging of rats. Nucl Med Biol. 59:1-8.

Salomone S, Caraci F, Leggio GM, Fedotova J, Drago F (2012) New pharmacological strategies for treatment of Alzheimer's disease: focus on disease modifying drugs. Br J Clin Pharmacol. 73:504-17.

Samnick S, Ametamey S, Leenders KL, Vontobel P, Quack G, Parsons CG, Neu H, Schubiger PA (1998) Electrophysiological study, biodistribution in mice, and preliminary PET evaluation in a rhesus monkey of 1-amino-3-[^{18}F]fluoromethyl-5-methyl-adamantane (^{18}F-MEM): a potential radioligand for mapping the NMDA-receptor complex. Nucl Med Biol. 25:323-30.

Selkoe DJ (1991) The molecular pathology of Alzheimer's disease. Neuron. 6:487–98.

Selkoe DJ (2004) Cell biology of protein misfolding: the examples of Alzheimer's and Parkinson's diseases. Nat Cell Biol. 6:1054-61.

Valis M, Herman D, Vanova N, Masopust J, Vysata O, Hort J, Pavelek Z, Klimova B, Kuca K, Misik J, Zdarova Karasova J (2019) The concentration of Memantine in the cerebrospinal fluid of alzheimer's disease patients and its consequence to oxidative stress biomarkers. Front Pharmacol. 10:943.

Van Dam D, Abramowski D, Staufenbiel M, De Deyn PP (2005) Symptomatic effect of donepezil, rivastigmine, galantamine and memantine on cognitive deficits in the APP23 model.Psychopharmacology (Berl). 180:177-90.

Van Dam D, De Deyn PP (2006) Cognitive evaluation of disease-modifying efficacy of galantamine and memantine in the APP23 model. Eur Neuropsychopharmacol. 16:59-69.

Villard V, Espallergues J, Keller E, Alkam T, Nitta A, Yamada K, Nabeshima T, Vamvakides A, Maurice T (2009) Anti-amnesic and neuroprotective effects of the aminotetrahydrofuran derivative ANAVEX1-41 against amyloid ß$_{25-35}$-induced toxicity in mice. Neuropsychopharmacology. 34:1552-66.

Villard V, Espallergues J, Keller E, Vamvakides A, Maurice T (2011) Anti-amnesic and neuroprotective potentials of the mixed muscarinic receptor/sigma$_1$ (σ_1) ligand ANAVEX2-73, a novel aminotetrahydrofuran derivative. J Psychopharmacol. 25:1101-17.

Wang R, Reddy PH (2017) Role of Glutamate and NMDA Receptors in Alzheimer's Disease. J Alzheimers Dis. 57:1041-1048.

Wang X, Blanchard J, Grundke-Iqbal I, Iqbal K (2015) Memantine attenuates Alzheimer's disease-like pathology and cognitive impairment. PLoS One. 10:e0145441.

Xia P, Chen HS, Zhang D, Lipton SA (2010) Memantine preferentially blocks extrasynaptic over synaptic NMDA receptor currents in hippocampal autapses. J Neurosci. 30:11246-50.

Zajaczkowski W, Quack G, Danysz W (1996) Infusion of (+)-MK-801 and memantine - contrasting effects on radial maze learning in rats with entorhinal cortex lesion. Eur J Pharmacol. 296:239-46.

Legends for the figures

Figure 1. Anti-amnesic effect of Memantine (**a**, **c**, **e**, **g**) and FENM (**b**, **d**, **f**, **h**) on $A\beta_{25-35}$-induced learning impairments in mice: (**a**, **b**) spontaneous alternation performance, (**c**, **d**) passive avoidance, and (**e-h**) object recognition test. Animals received Memantine or FENM (0.1-10 mg/kg IP) 30 min before the Y-maze test session, passive avoidance training session, or session 2 of the object recognition test. For the object recognition test, exploration preferences are calculated with the duration of contacts in session 2, with 2 identical objects (e, f) and in session 3 with a novel object (g, h). Data show mean ± SEM in (a, b, e-h) and median and interquartile range in (c, d). ANOVA: $F_{(6,83)} = 2.62$, $p < 0.05$, in (a); $F_{(6,89)} = 4.94$, $p < 0.001$, in (b). Kruskal-Wallis ANOVA: $H = 23.4$, $p < 0.001$, in (c); $H = 19.5$, $p < 0.01$, in (d). * $p < 0.05$, ** $p < 0.01$, *** $p < 0.001$ *vs*. (Sc.Aß+V)-treated group; # $p < 0.05$, ## $p < 0.01$ *vs*. (V+$A\beta_{25-35}$)-treated group; Dunnett's test in (a, b), Dunn's test in (c, d). ° $p < 0.05$, °° $p < 0.01$, °°° $p < 0.001$ *vs*. 50% level, one-sample *t*-test in (g, h).

Figure 2. Effects of Memantine and FENM, administered at 0.3 mg/kg IP, on $A\beta_{25-35}$-induced learning impairments: (**a-c**) spatial reference memory in the water-maze in mice; (**d-i**) topographic memory in the Hamlet test. (**a**) Acquisition of Veh-treated and $A\beta_{25-35}$-injected animals. (**b**) Acquisition of animals receiving Memantine or FENM, 0.3 mg/kg IP, 30 min before the training trials sessions (anti-amnesia). (**c**) time spent in the training (T) or the others (o) quadrants for each experimental group. °° $p < 0.01$, °°° $p < 0.001$ *vs*. 15 s; one-sample t-test; *** $p < 0.001$ *vs*. o quadrants; Student-'s *t*-test. Hamlet probe test data were analyzed in terms of errors (**d-f**) and latencies (**g-i**) to reach the Drink house. (**d**, **g**) Probe test performed 72 h after Hamlet training. (**e**, **h**) Probe test performed one week after the ICV injection of $A\beta_{25-35}$ and 30 min after IP injection of Memantine or FENM. (**f**, **i**) Disorientation index calculations for errors (f) or latencies (i). * p < 0.05, ** $p < 0.01$ *vs*. NWD, paired *t*-test; ° $p < 0.05$ *vs*. zero level, one-sample *t*-test.

Figure 3. Protective effect of Memantine (**a, c, e, g**) and FENM (**b, d, f, h**), administered IP, on $A\beta_{25-35}$-induced learning impairments in mice: (**a, b**) spontaneous alternation performance, (**c, d**) passive avoidance, and (**e-h**) object recognition tests. Animals received Memantine or FENM (0.1-10 mg/kg ip) o.d. between day 1 to 7 and injections stopped 24 h before the first behavioral session. For the object recognition test, exploration preferences are calculated with the duration of contacts in session 2, with 2 identical objects (e, f) and in session 3 with a novel object (g, h). Data show mean ± SEM in (a, b, e-h) and median and interquartile range in (c, d). ANOVA: $F_{(6,93)} = 5.16$, $p < 0.0001$, in (a); $F_{(6,90)} = 6.21$, $p < 0.0001$, in (b). Kruskal-Wallis ANOVA: $H = 21.6$, $p < 0.01$, in (c); $H = 29.8$, $p < 0.001$, in (d). * $p < 0.05$, ** $p < 0.01$, *** p < 0.001 *vs*. (V+V)-treated group; # $p < 0.05$, ## $p < 0.01$ *vs*. (V+$A\beta_{25-35}$)-treated group; Dunnett's test in (a, b), Dunn's test in (c, d). ° $p < 0.05$, °° $p < 0.01$, °°° $p < 0.001$ *vs*. 50% level, one-sample *t*-test in (g, h).

Figure 4. Protective effects of Memantine and FENM, administered at 0.3 mg/kg IP, on $A\beta_{25-35}$-induced learning impairments: spatial reference memory in the water-maze in mice. (**a**) Acquisition of Veh-treated and $A\beta_{25-35}$-injected animals. (**b**) Acquisition of animals receiving Memantine or FENM, 0.3 mg/kg IP, after the $A\beta_{25-35}$ peptide on day 1 and started training on day 8 (neuroprotection). (**c**) time spent in the training (T) or the others (o) quadrants for each experimental group. °° $p < 0.01$, °°° $p < 0.001$ *vs*. 15 s; one-sample *t*-test; *** $p < 0.001$ *vs*. o quadrants; Student-'s *t*-test.

Figure 5. Protective effects of Memantine and FENM, administered at 0.3 mg/kg IP, on $A\beta_{25-35}$-induced (**a-**c) oxidative stress and mitochondrial alteration and (**d**) Iba-1, (**e**) GFAP, (**f**) IL-6, (**g**) TNFα, (**h**) Bcl-2, and (**i**) Bax contents measured by ELISA in the mouse hippocampus. (**a, b**) cytochrome c release from mitochondria to the cytosol in cortex extracts. (a) Typical blots showing OXPHOS mitochondrial marker and cytochrome c labeling. Normalization was done with stain free total protein content in each band. (b) Quantification. (c) Measure of lipid

peroxidation level in mouse cortex extracts. Elisa assays were done 16 days after ICV injection in (d, e, h, i) or 5 days after ICV injection in (f, g). (**j**) Bax/Bcl-2 ratio. ANOVA: $F_{(3,31)} = 3.05$, $p < 0.05$ in (b). $F_{(3,21)} = 4.33$, $p < 0.05$; $F_{(3,22)} = 2.53$, $p > 0.05$ in (d); $F_{(3,21)} = 1.06$, $p > 0.05$ in (e); $F_{(3,31)} = 3.06$, $p < 0.05$ in (f); $F_{(3,31)} = 2.10$, $p > 0.05$ in (g); $F_{(3,22)} = 2.00$, $p > 0.05$ in (h); $F_{(3,22)} = 3.37$, $p < 0.05$ in (i); $F_{(3,22)} = 0.763$, $p > 0.05$ in (j). * $p < 0.05$, *** $p < 0.001$ *vs*. (V+V)-treated group; # $p < 0.05$ *vs*. (V+Aβ_{25-35})-treated group; Dunnett's test.

Figure 6. Protective effects of Memantine and FENM, administered at 0.3 mg/kg IP, on cell loss in the CA1 hippocampal pyramidal cell layer of Aβ_{25-35}-treated mice using cresyl violet staining: (**a-d**) typical micrographs and (**e**) quantifications of the number of viable cells and (**f**) the cell layer thickness. 3-6 slices were counted per animals. ANOVA: $F_{(3,113)} = 9.08$, $p < 0.0001$ in (i); $F_{(3,113)} = 8.35$, $p < 0.0001$ in (j). * $p < 0.05$, ** $p < 0.01$ *vs*. the (V+V)-treated group; # $p < 0.05$, ## $p < 0.01$ *vs*. the (Aβ_{25-35}+V)-treated group; Dunnett's test. (**g**) Anatomical localization of the hippocampal and cortical areas analyzed in the mouse brain (cresyl violet staining at low magnification). Left: Areas; right: anatomical distribution. Abbreviations: CA1~CA3, pyramidal cell layers; DG, dentate gyrus; PoDG, polymorph layer of the DG; Mol, molecular layer of the DG; LMol, lacunosum molecular layer; Rad, stratum radiatum; RSG, retrosplenial granular cortex; RSA, retroplenial agranular cortex; LPtA, lateral parietal associative cortex; V2L, lateral area of the 2nd visual cortex; Au, 2nd auditory cortex; Thal, thalamus. Scale bars = 50 µm in (a), 500 µm in (g).

Figure 7. Protective effects of Memantine and FENM, administered at 0.3 mg/kg IP, on the astroglial reaction in the hippocampus of Aβ_{25-35}-treated mice using GFAP immunolabeling: (**a-e**) stratum radiatum, (**f-j**) molecular layer, and (**k-o**) polymorph layer with (**a-d, f-i, k-n**) typical immunofluorescence micrographs (blue: DAPI, green: GFAP) and (**e, j, o**) quantifications. Coronal 25 µm thick sections were stained with anti-GFAP antibody and three areas of the hippocampus analyzed as shown in Figure 8g. Scale bar in (a) = 50 µm. ANOVA: $F_{(3,22)} = 5.06$, $p < 0.01$, in (e); $F_{(3,23)} = 4.50$, $p < 0.05$, in (j); $F_{(3,23)} = 3.24$, $p < 0.05$, in (o). * $p < 0.05$, *** $p <$

0.001 *vs*. the (V+V)-treated group; # $p < 0.05$, ## $p < 0.01$ *vs*. the ($A\beta_{25-35}$+V)-treated group; Dunnett's test.

Figure 8. Protective effects of Memantine and FENM, administered at 0.3 mg/kg IP, on the microglial reaction in the hippocampus of $A\beta_{25-35}$-treated mice using Iba-1 immunolabeling: (**a-e**) stratum radiatum, (**f-j**) molecular layer, and (**k-o**) polymorph layer with (**a-d, f-i, k-n**) typical immunofluorescence micrographs (Blue: DAPI, Red: Iba-1) and (**e, j, o**) quantifications. Coronal 25 µm thick sections were stained with anti-Iba-1 antibody and three areas of the hippocampus analyzed as shown in Figure 6g. Scale = 50 µm. ANOVA: $F_{(3,23)} = 3.22$, $p < 0.05$, in (e); $F_{(3,22)} = 2.86$, $p > 0.05$, in (j); $F_{(3,23)} = 3.38$, $p < 0.05$, in (o). * $p < 0.05$, *** $p < 0.001$ *vs*. the (V+V)-treated group; # $p < 0.05$, ## $p < 0.01$ *vs*. the ($A\beta_{25-35}$+V)-treated group; Dunnett's test.

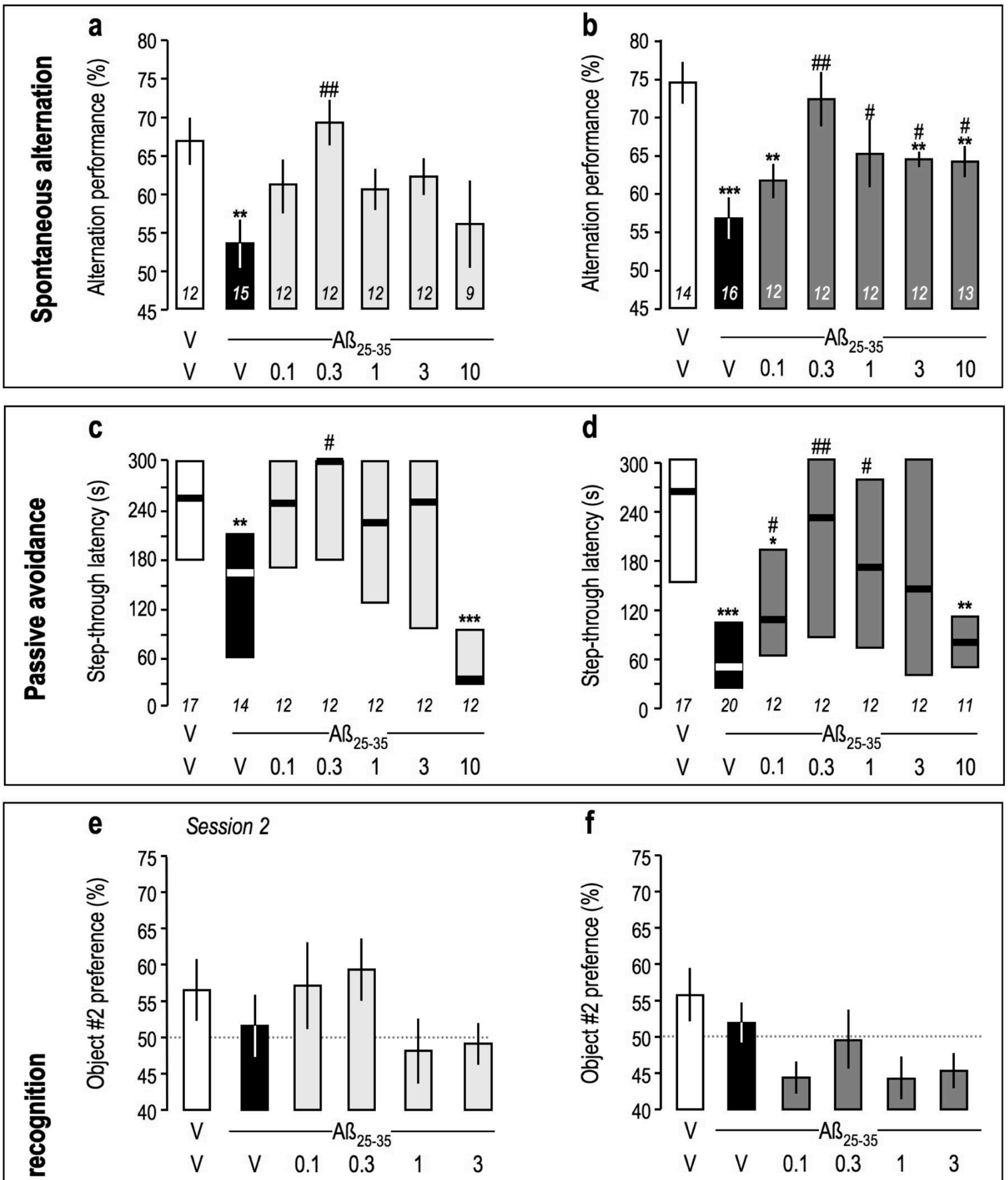
Spontaneous alternation
a
Alternation performance (%)
80
75
70
65
60
55
50
45
12
15
12
12
12
12
9
**
##
V
V
V
Aß25-35
0.1
0.3
1
3
10
b
Alternation performance (%)
14
16
12
12
12
12
13
***
**
##
#
#
**
Passive avoidance
c
Step-through latency (s)
300
240
180
120
60
0
17
14
12
12
12
12
12
**
#
***
d
Step-through latency (s)
17
20
12
12
12
12
11
***
#
*
##
#
**
Object recognition
e
Session 2
Object #2 preference (%)
75
70
65
60
55
50
45
40
f
Object #2 prefernce (%)
g
Session 3
Novel object preference (%)
10
11
11
8
8
12
oo
o
o
oo
h
Novel object preference (%)
13
15
12
12
12
12
ooo
oo
ooo
Memantine (mg/kg IP)
FENM (mg/kg IP)

Place learning in the water-maze

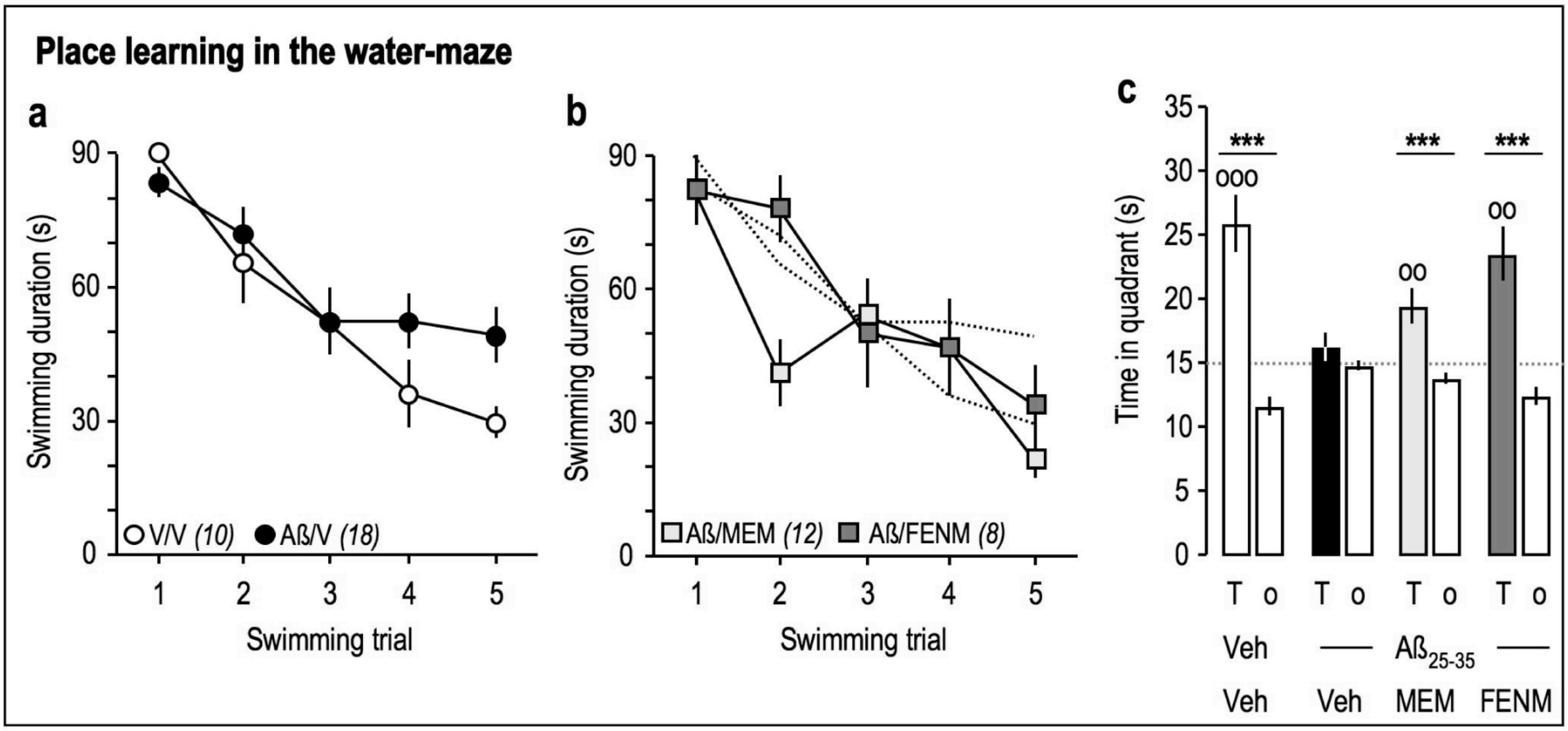

Topographic memory in the Hamlet

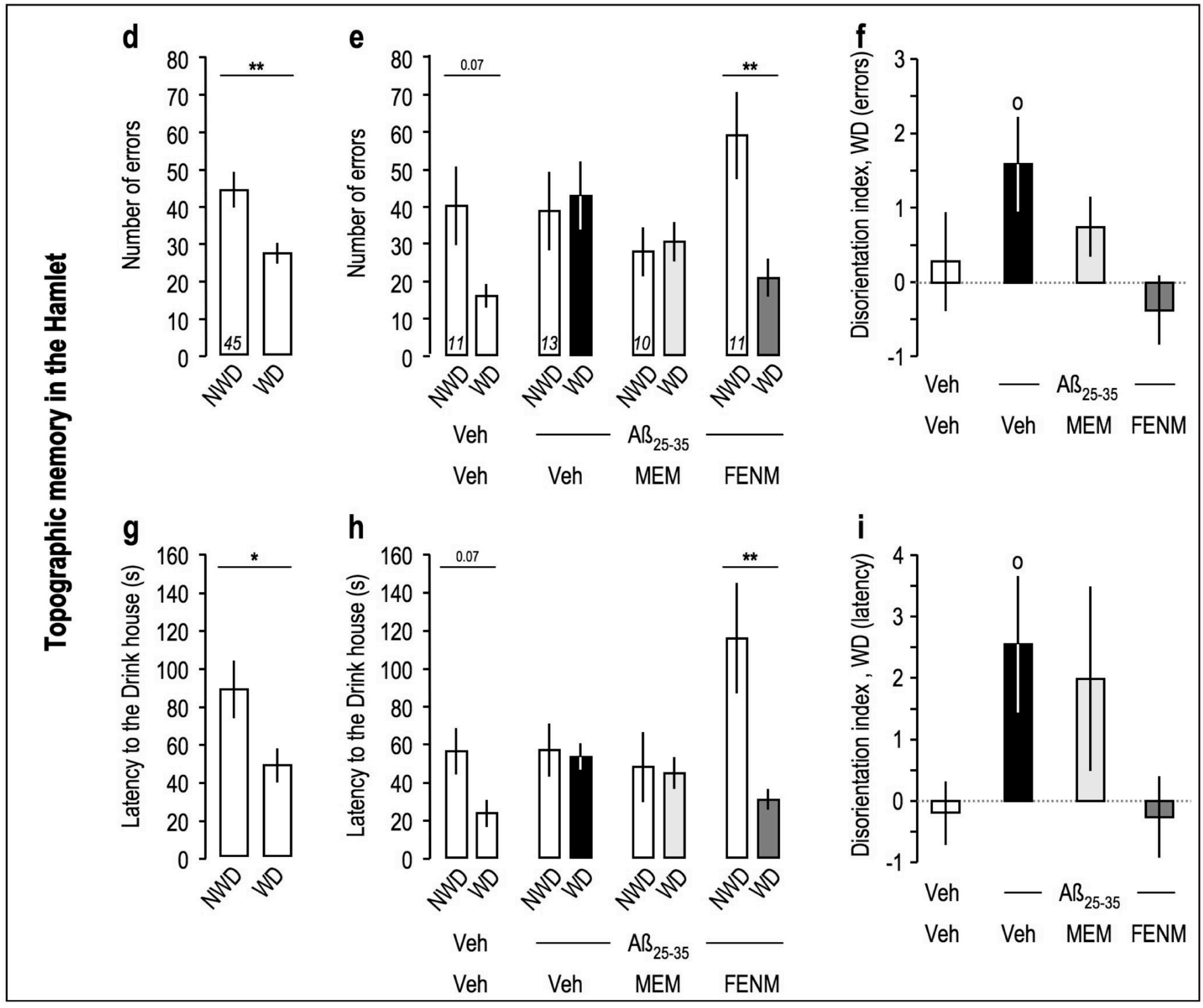

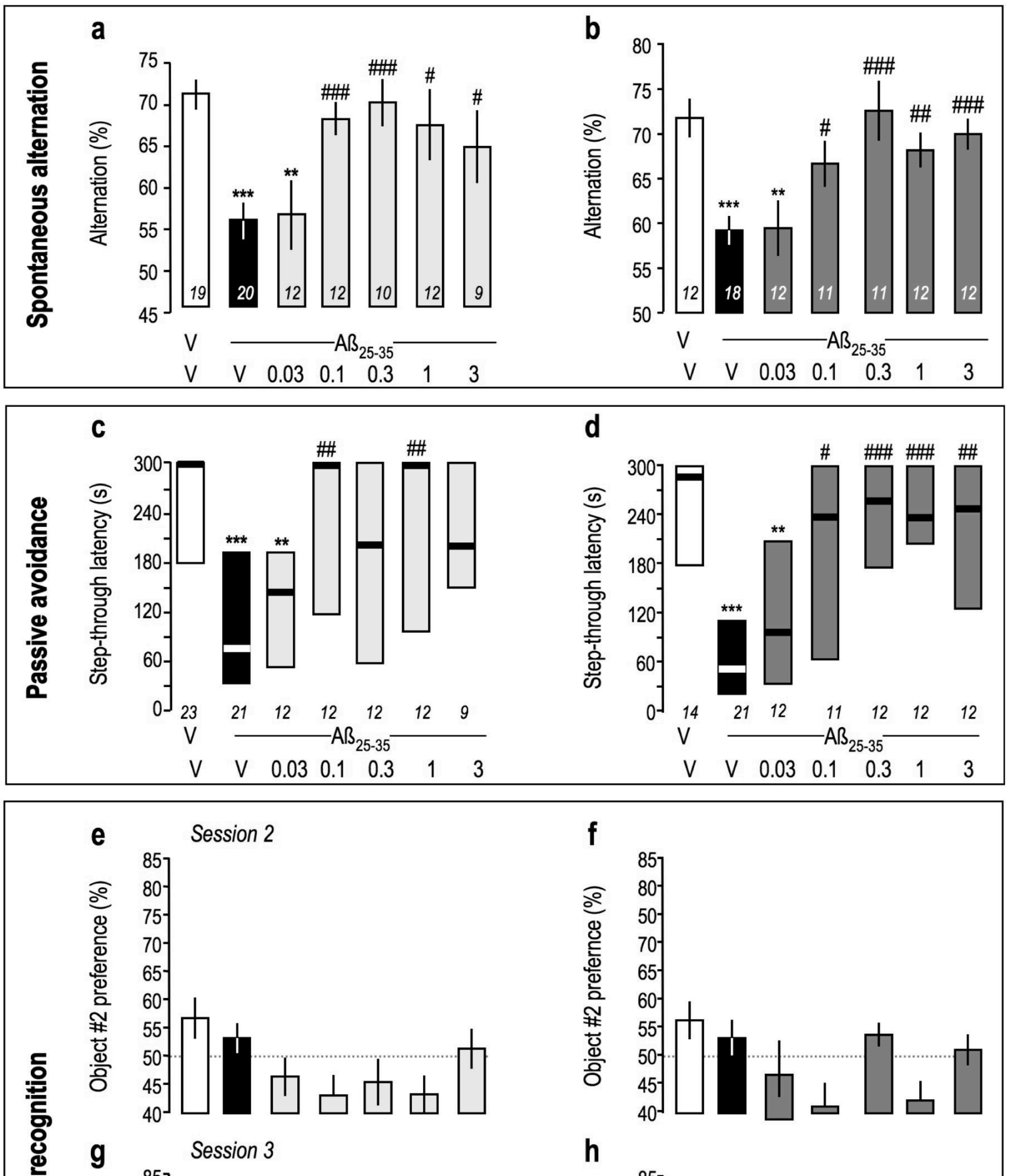
Spontaneous alternation
a
Alternation (%)
75
70
65
60
55
50
45
19
20
12
12
10
12
9
***
**
###
###
#
#
V
Aß25-35
V V 0.03 0.1 0.3 1 3
b
Alternation (%)
80
75
70
65
60
55
50
12
18
12
11
11
12
12
***
**
#
###
##
###
V
Aß25-35
V V 0.03 0.1 0.3 1 3
Passive avoidance
c
Step-through latency (s)
300
240
180
120
60
0
23
21
12
12
12
12
9
***
**
##
##
V
Aß25-35
V V 0.03 0.1 0.3 1 3
d
Step-through latency (s)
300
240
180
120
60
0
14
21
12
11
12
12
12
***
**
#
###
###
##
V
Aß25-35
V V 0.03 0.1 0.3 1 3
Object recognition
e
Session 2
Object #2 preference (%)
85
80
75
70
65
60
55
50
45
40
f
Object #2 prefernce (%)
85
80
50
70
65
60
55
50
45
40
g
Session 3
Novel object preference (%)
85
80
75
70
65
60
55
50
45
40
000
o
oo
14
15
12
12
12
12
12
V
Aß25-35
V V 0.03 0.1 0.3 1 3
h
Novel object preference (%)
85
80
75
70
65
60
55
50
45
40
000
o
oo
o
o
18
14
12
12
12
12
12
V
Aß25-35
V V 0.03 0.1 0.3 1 3
Memantine (mg/kg IP)
FENM (mg/kg IP)

Figure 4

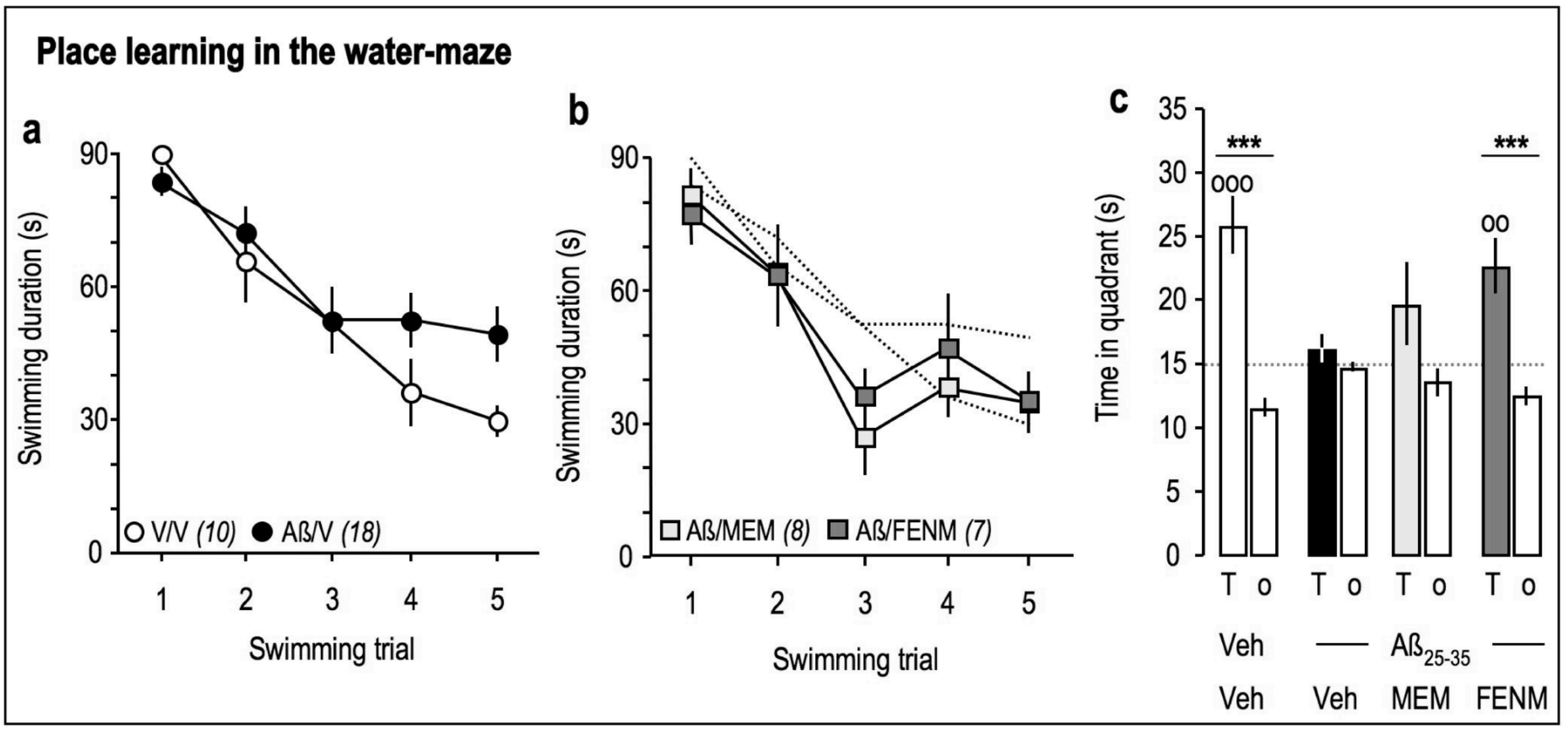
Place learning in the water-maze
a
Swimming duration (s)
90
60
30
0
V/V (10)
Aß/V (18)
1
2
3
4
5
Swimming trial
b
Swimming duration (s)
90
60
30
0
Aß/MEM (8)
Aß/FENM (7)
1
2
3
4
5
Swimming trial
c
Time in quadrant (s)
35
30
25
20
15
10
5
0
***
ooo
***
oo
T o T o T o T o
Veh
Aß25-35
Veh Veh MEM FENM

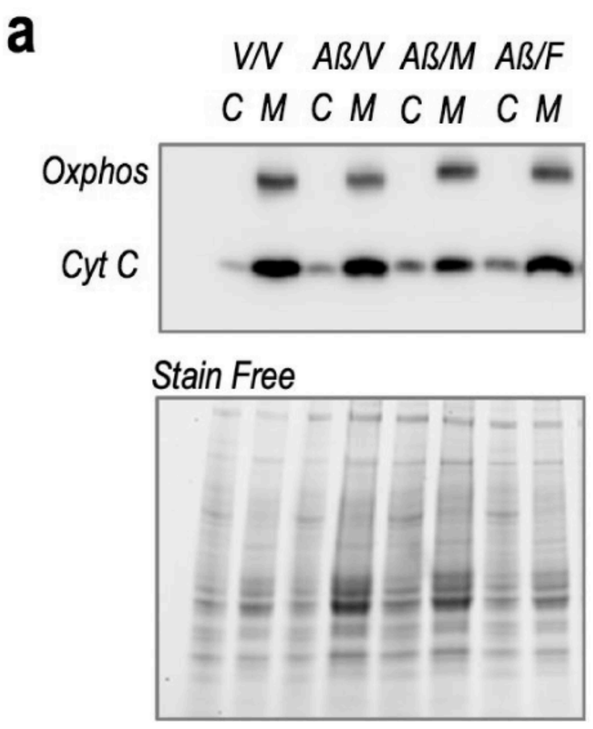
a
V/V Aß/V Aß/M Aß/F
C M C M C M C M
Oxphos
Cyt C
Stain Free

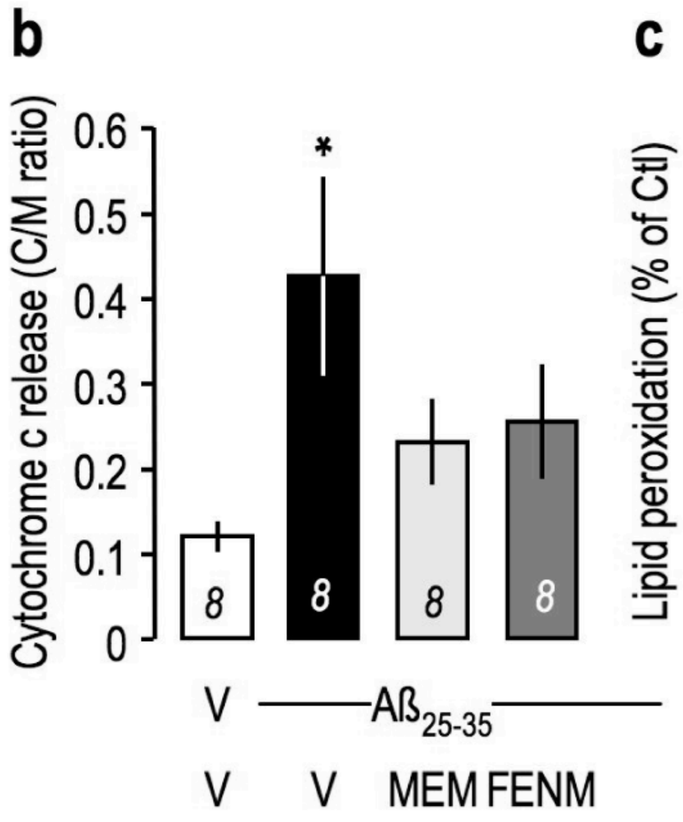
b
Cytochrome c release (C/M ratio)
0.6
0.5
0.4
0.3
0.2
0.1
0
*
8
8
8
8
V — Aß25-35
V V MEM FENM

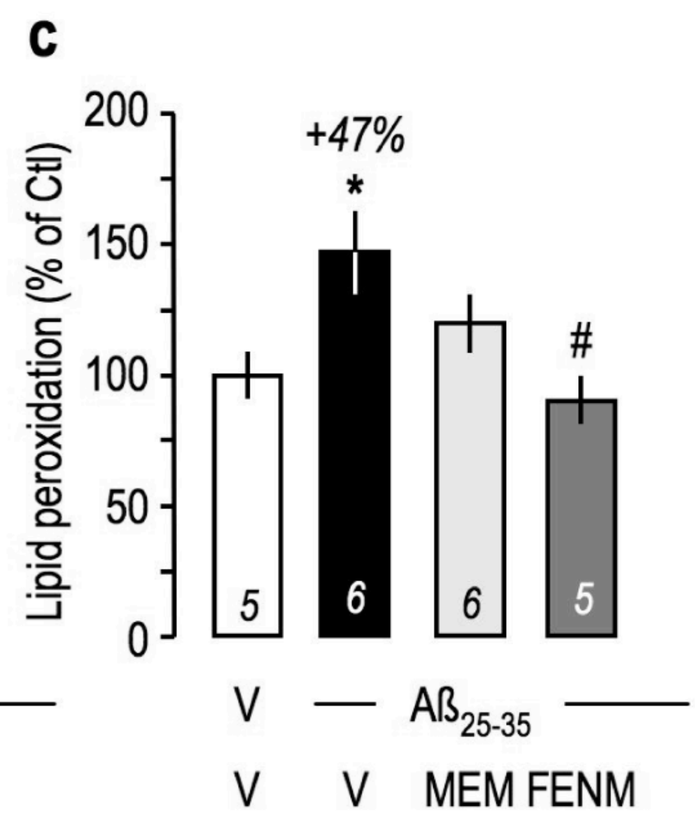
c
Lipid peroxidation (% of Ctl)
200
150
100
50
0
+47%
*
#
5
6
6
5
V — Aß25-35
V V MEM FENM

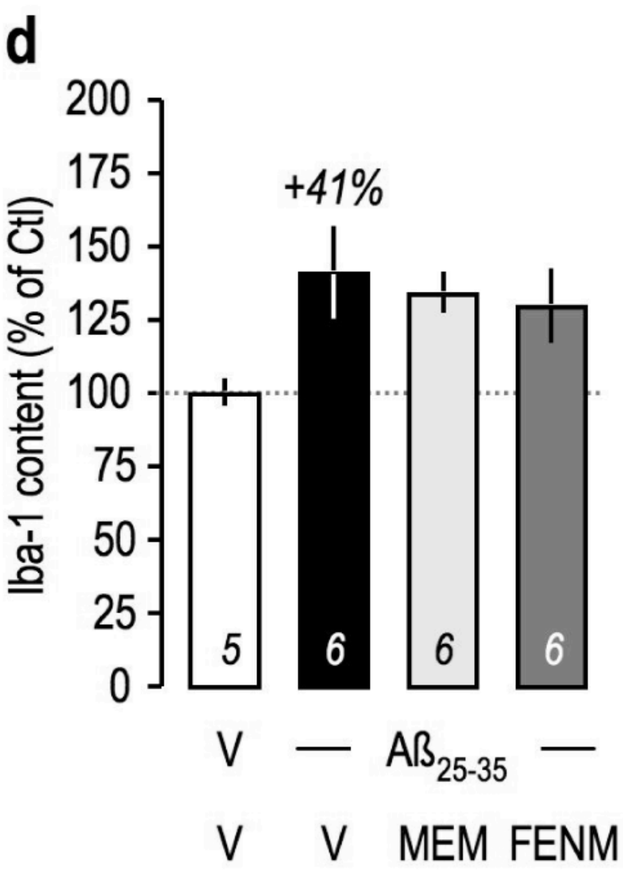
d
Iba-1 content (% of Ctl)
200
175
150
125
100
75
50
25
0
+41%
5
6
6
6
V — Aß25-35 —
V V MEM FENM

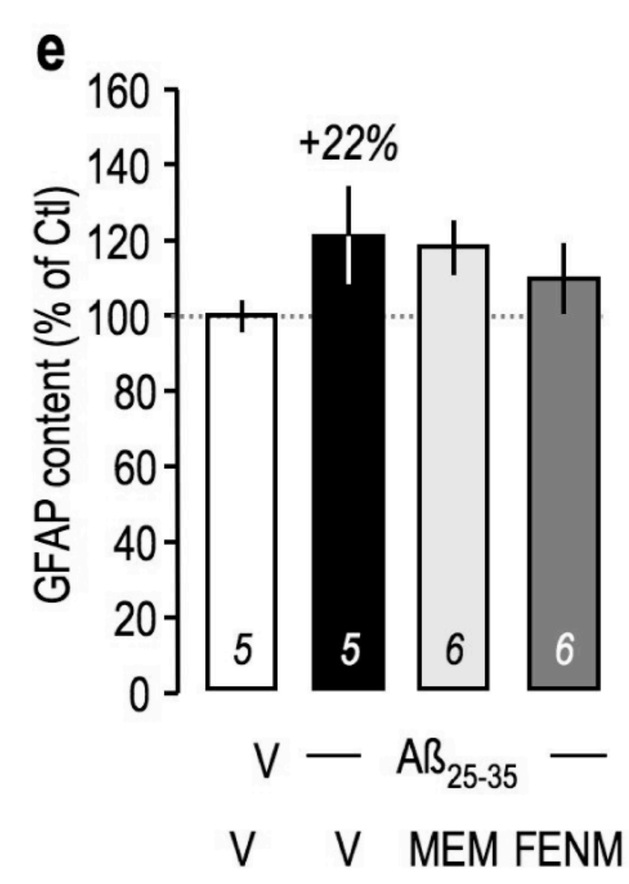
e
GFAP content (% of Ctl)
160
140
120
100
80
60
40
20
0
+22%
5
5
6
6
V — Aß25-35 —
V V MEM FENM

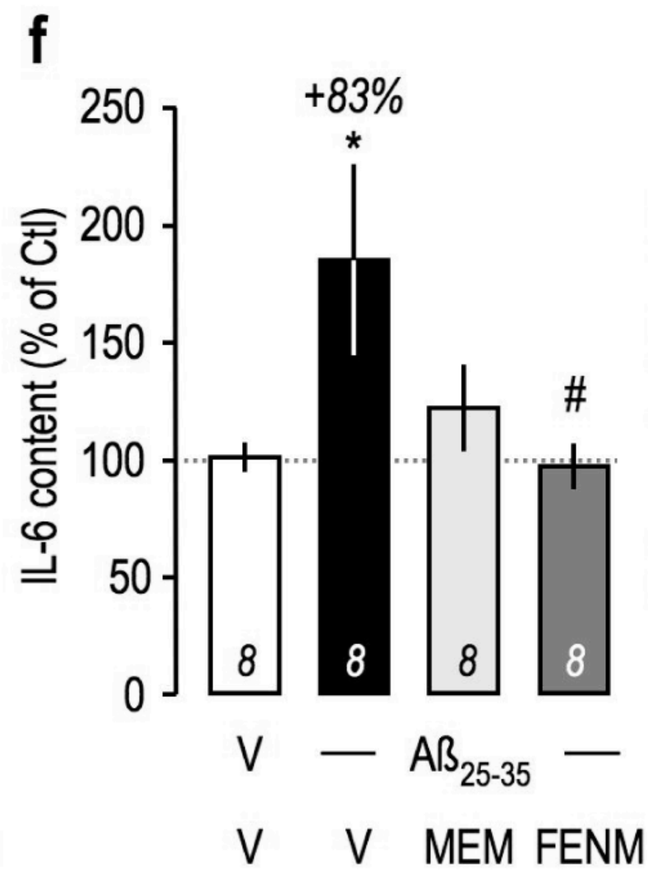
f
IL-6 content (% of Ctl)
250
200
150
100
50
0
+83%
*
#
8
8
8
8
V — Aß25-35 —
V V MEM FENM

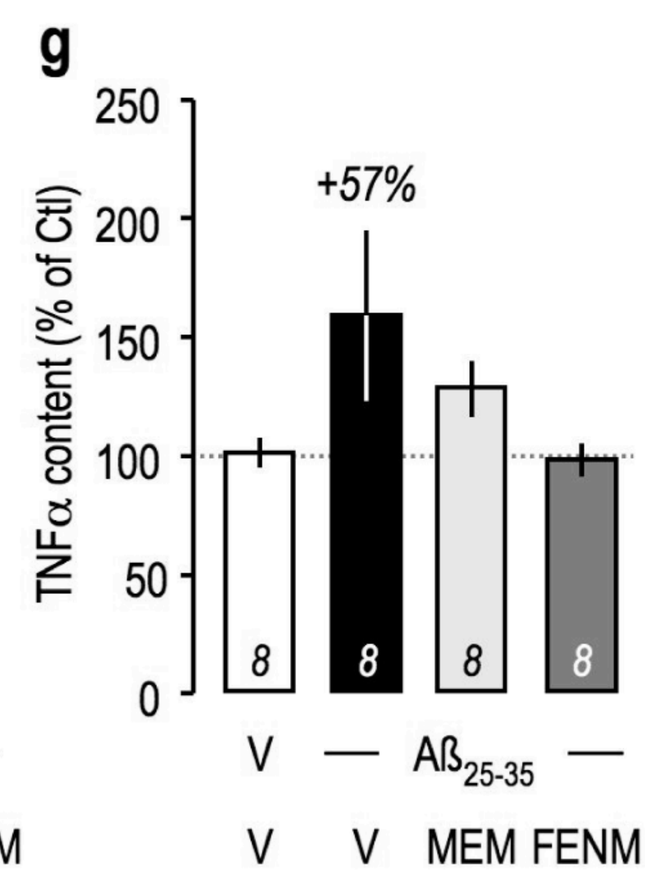
g
TNFα content (% of Ctl)
250
200
150
100
50
0
+57%
8
8
8
8
V — Aß25-35 —
V V MEM FENM
Drugs (0.3 mg/kg IP)

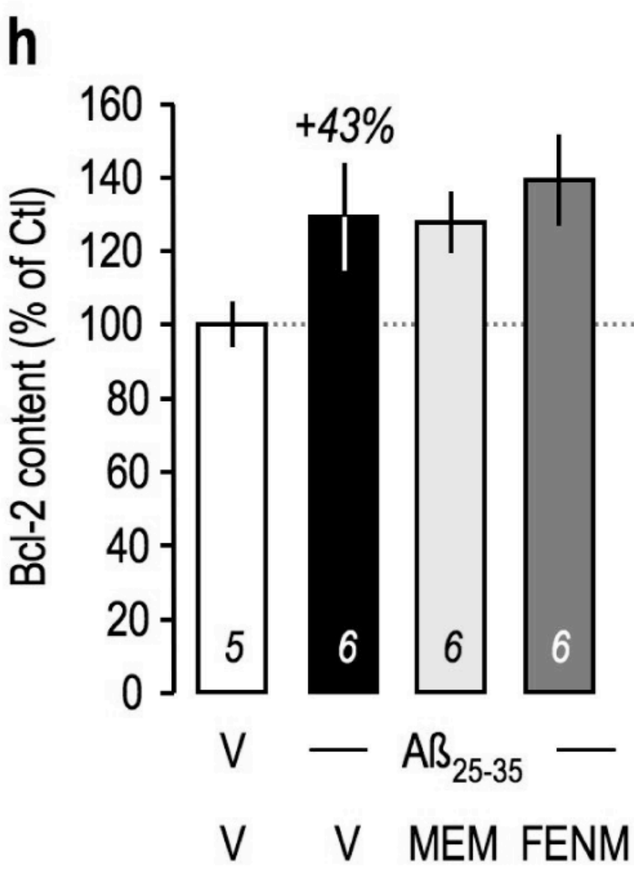
h
Bcl-2 content (% of Ctl)
160
140
120
100
80
60
40
20
0
+43%
5
6
6
6
V — Aß25-35 —
V V MEM FENM
Drugs (0.3 mg/kg IP)

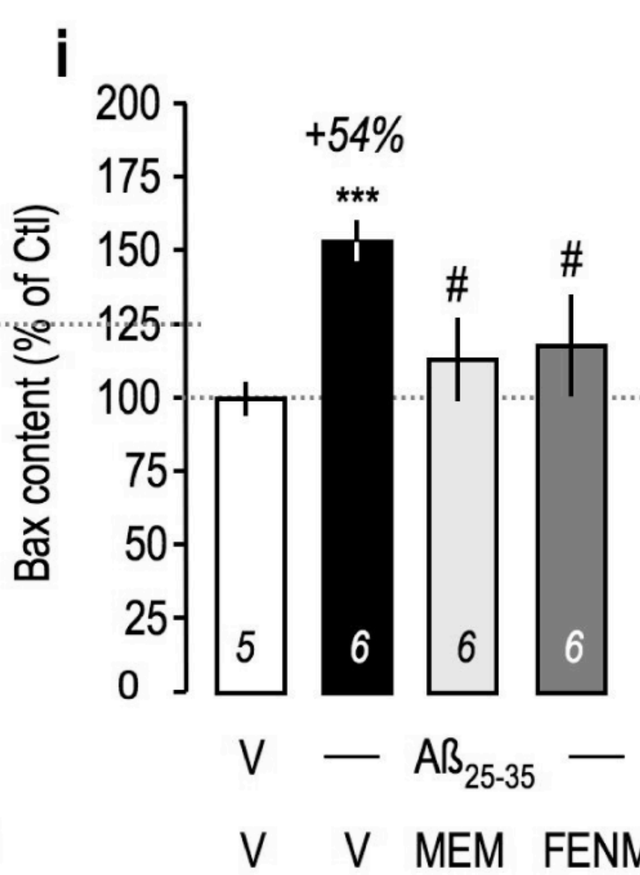
i
Bax content (% of Ctl)
200
175
150
125
100
75
50
25
0
+54%
***
#
#
5
6
6
6
V — Aß25-35 —
V V MEM FENM
Drugs (0.3 mg/kg IP)

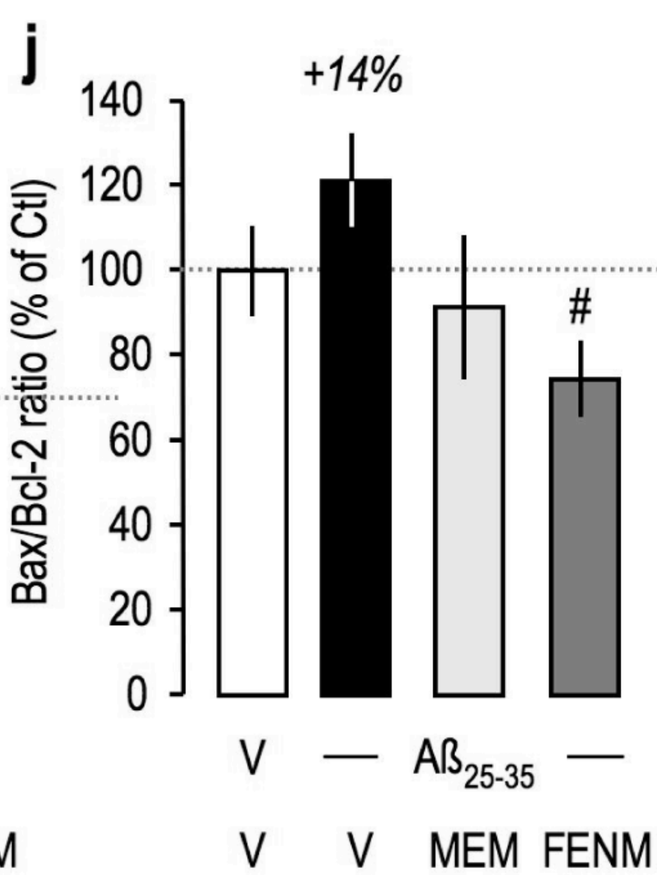
j
Bax/Bcl-2 ratio (% of Ctl)
140
120
100
80
60
40
20
0
+14%
#
V — Aß25-35 —
V V MEM FENM
Drugs (0.3 mg/kg IP)

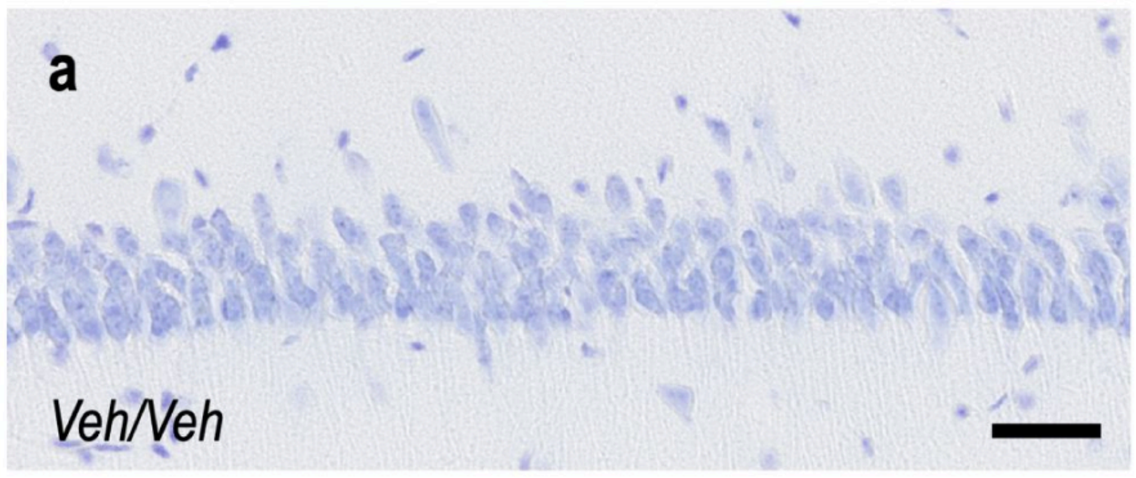
a
Veh/Veh

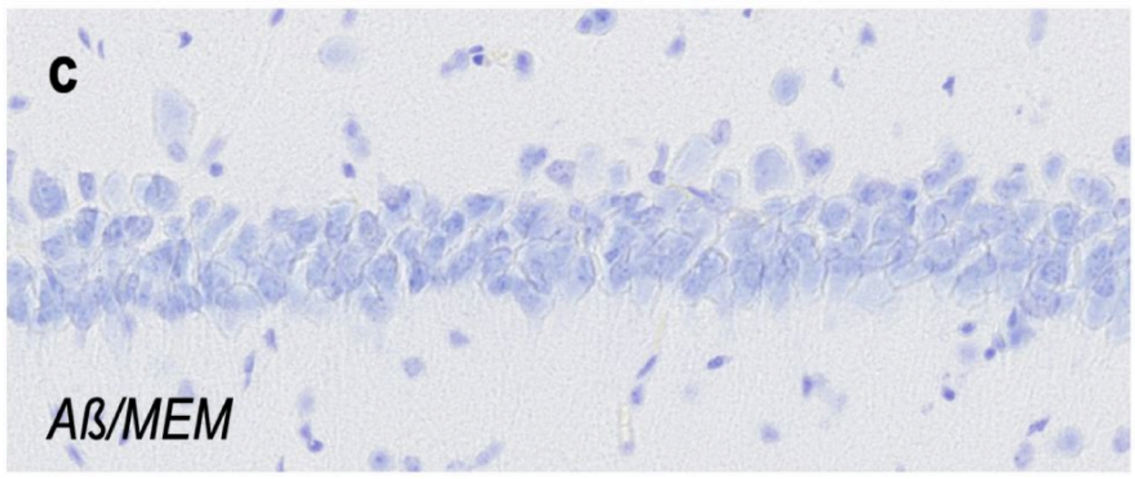
c
Aß/MEM

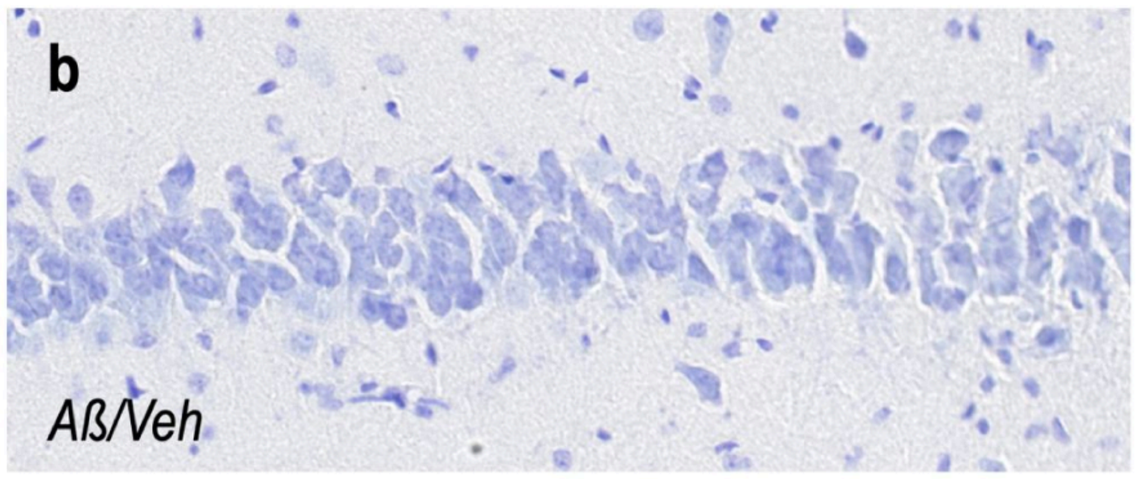
b
Aß/Veh

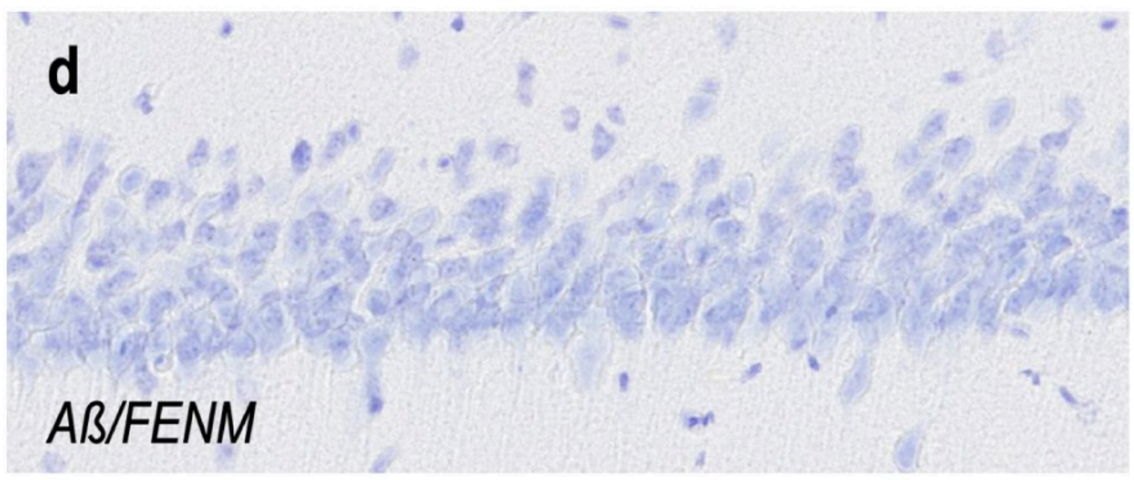
d
Aß/FENM

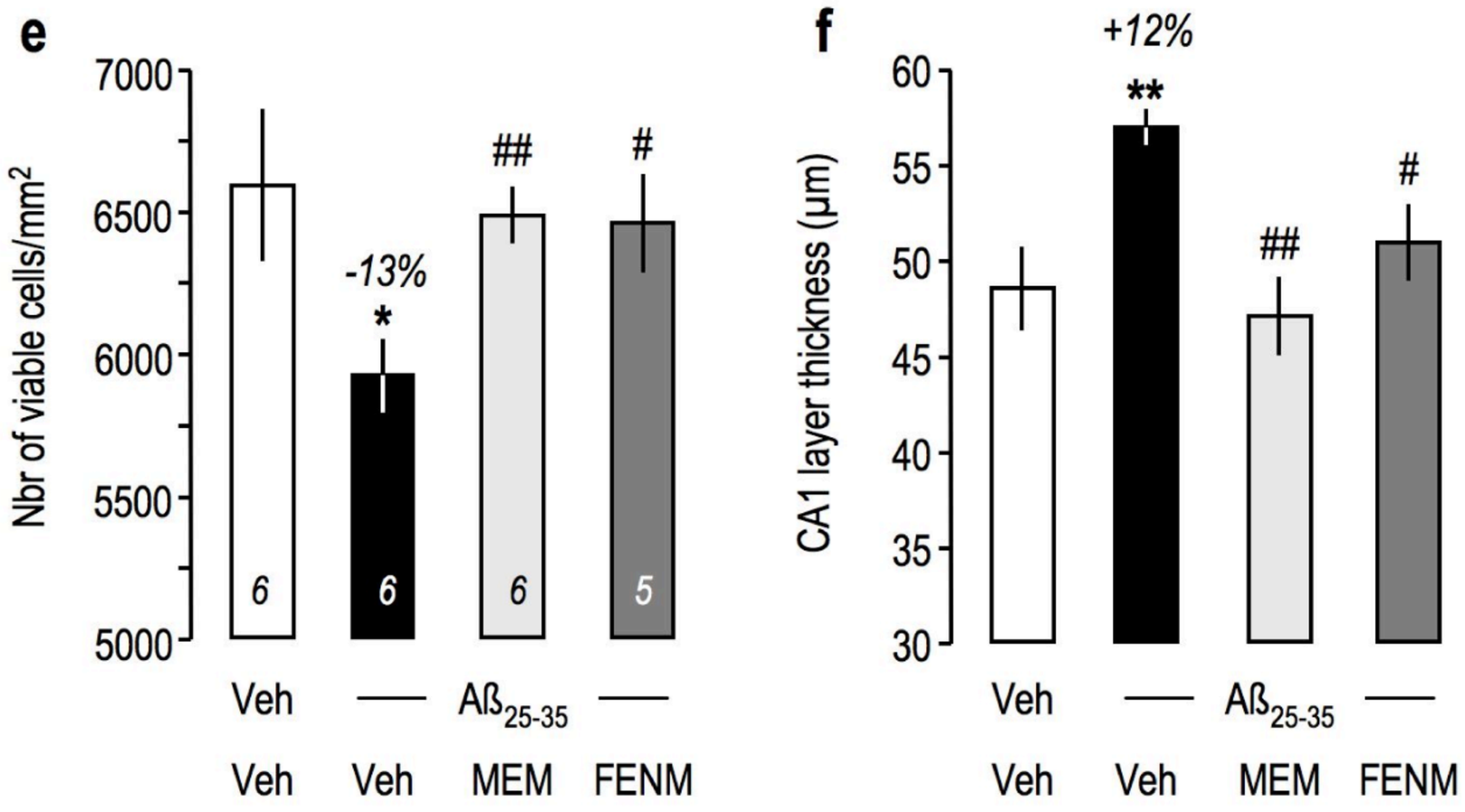
e
Nbr of viable cells/mm²
7000
6500
6000
5500
5000
-13%
*
##
#
6
6
6
5
Veh
Aß25-35
Veh
Veh
MEM
FENM
f
CA1 layer thickness (µm)
60
55
50
45
40
35
30
+12%
**
##
#
Veh
Aß25-35
Veh
Veh
MEM
FENM

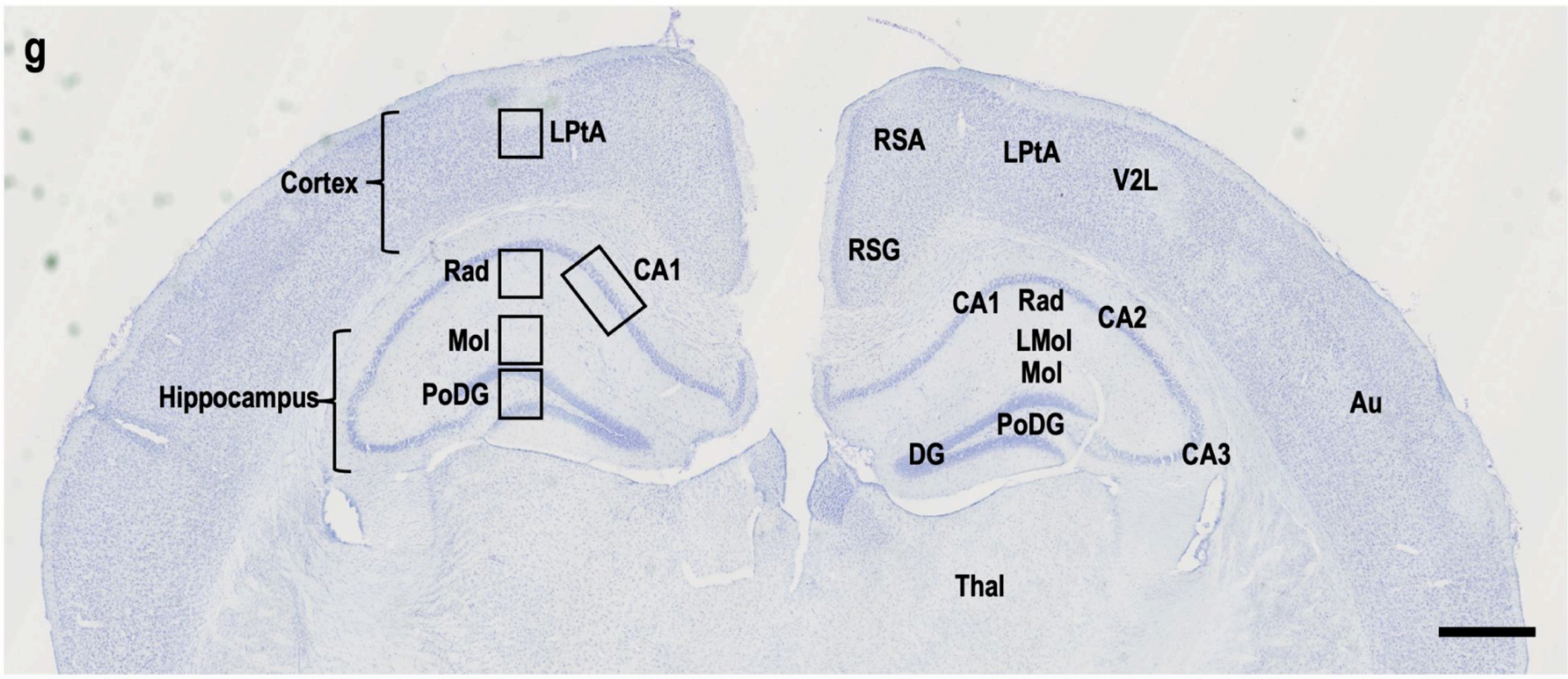
g
LPtA
Cortex
Rad
CA1
Mol
PoDG
Hippocampus
RSA
LPtA
V2L
RSG
CA1
Rad
LMol
Mol
CA2
PoDG
DG
CA3
Au
Thal

Figure 7

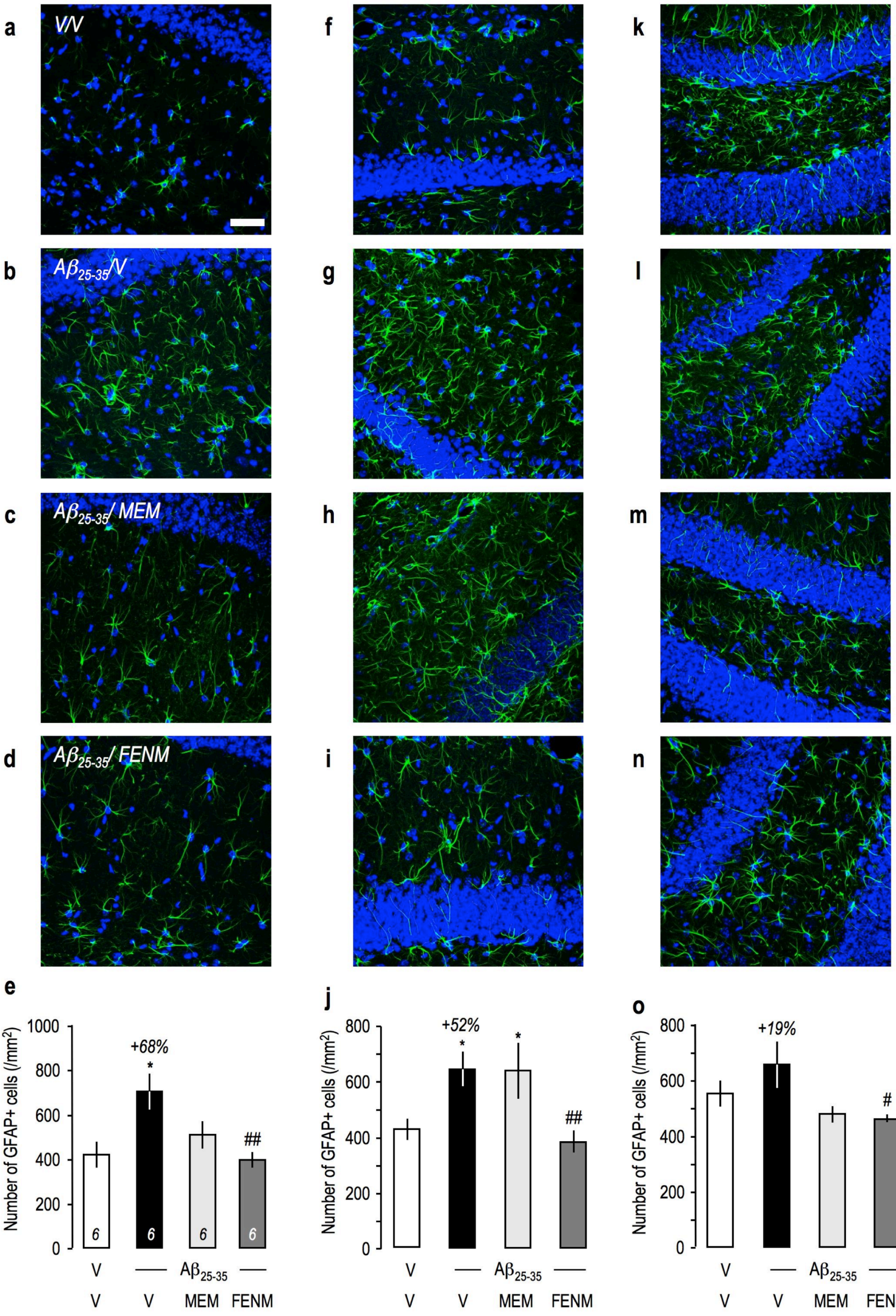
Rad
Mol
PoDG
a
V/V
f
k
b
Aβ25-35/V
g
l
c
Aβ25-35/ MEM
h
m
d
Aβ25-35/ FENM
i
n
e
Number of GFAP+ cells (/mm2)
1000
800
600
400
200
0
+68%
*
##
6
6
6
6
V
—
Aβ25-35
—
V
V
MEM
FENM
j
800
600
400
200
0
+52%
*
*
##
o
800
600
400
200
0
+19%
#

Figure 8

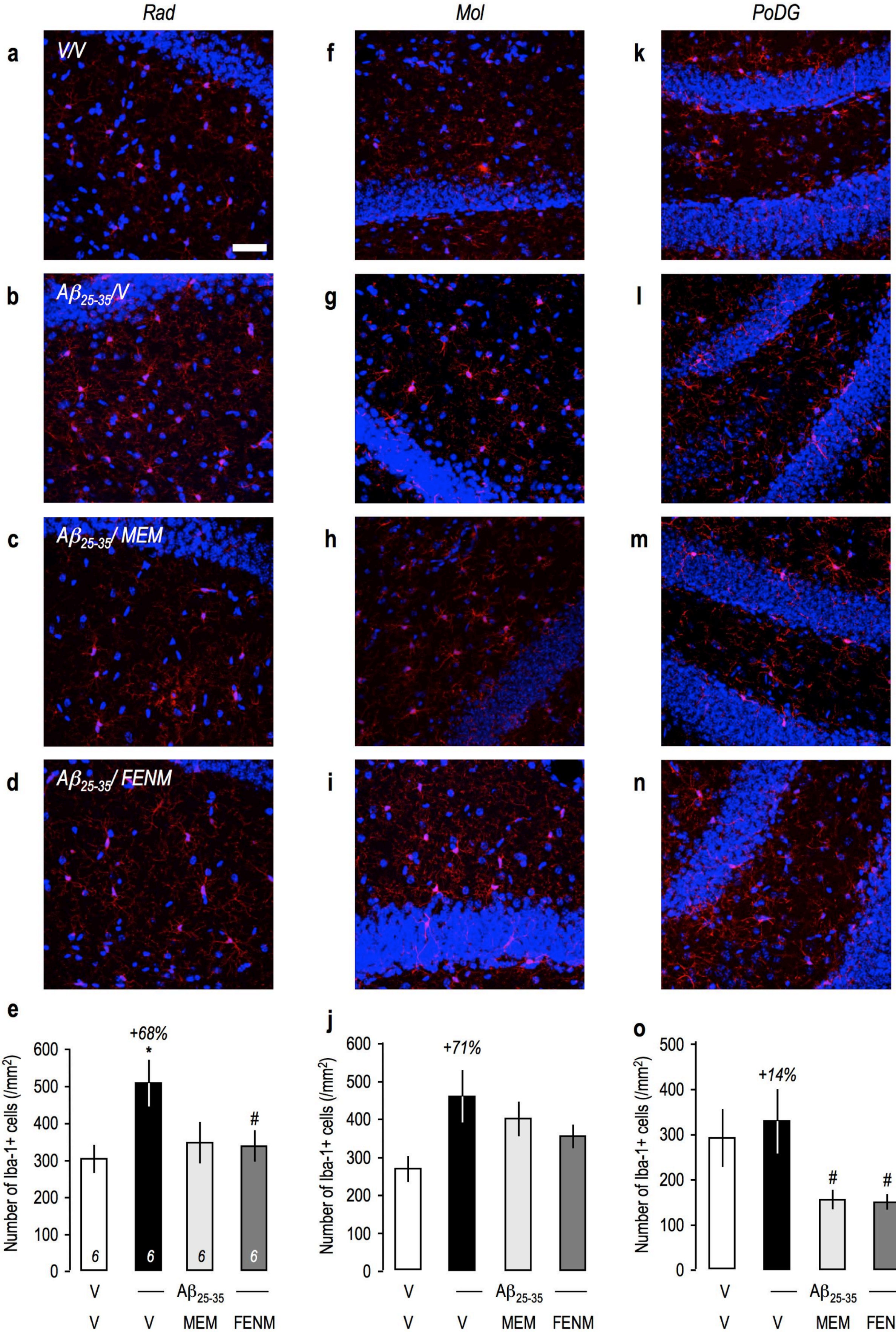
Rad
Mol
PoDG
a
V/V
f
k
b
Aβ25-35/V
g
l
c
Aβ25-35/ MEM
h
m
d
Aβ25-35/ FENM
i
n
e
+68%
*
#
Number of Iba-1+ cells (/mm2)
600
500
400
300
200
100
0
6
6
6
6
V
—
Aβ25-35
—
V
V
MEM
FENM
j
+71%
Number of Iba-1+ cells (/mm2)
600
500
400
300
200
100
0
V
—
Aβ25-35
—
V
V
MEM
FENM
o
+14%
#
#
Number of Iba-1+ cells (/mm2)
500
400
300
200
100
0
V
—
Aβ25-35
—
V
V
MEM
FENM

Supplementary Material

Supplementary Material and Methods

Behavioral tests

Spontaneous alternation in the Y-maze

The Y-maze is made of grey polyvinylchloride. Each arm is 40 cm long, 13 cm high, 3 cm wide at the bottom, 10 cm wide at the top, and converging at an equal angle. Each mouse was placed at the end of one arm and allowed to move freely through the maze during an 8 min session. The series of arm entries, including possible returns into the same arm, were checked visually. An alternation is defined as entries into all three arms on consecutive occasions. The number of maximum alternations is therefore the total number of arm entries minus two and the percentage of alternation was calculated as (actual alternations / maximum alternations) x 100 (Maurice et al., 1996; Meunier et al., 2006, 2013; Villard et al., 2009, 2011). Exclusion criteria are locomotion < 10 or percentage of alternation < 25% or > 90%. Animals showing these readouts are excluded from the calculations. Attrition is routinely < 5% in this test.

Step-through passive avoidance

The apparatus is a two-compartments (15 × 20 × 15 cm high) box with one illuminated with white polyvinylchloride walls and the other darkened with black polyvinylchloride walls and a grid floor. A guillotine door separates each compartment. A 60 W lamp positioned 40 cm above the apparatus lights up the white compartment during the experiment. Scrambled foot shocks (0.3 mA for 3 s) could be delivered to the grid floor using a shock generator scrambler (Lafayette Instruments, Lafayette, USA). The guillotine door was initially closed during the training session. Each mouse was placed into the white compartment. After 5 s, the door was raised. When the mouse entered the darkened compartment and placed all its paws on the grid floor, the door is closed and the foot shocks delivered for 3 s. The step-through latency (STL-Tg), that is, the latency spent to enter the darkened compartment, and the number of vocalizations were recorded. The retention test was carried out 24 h after training. Each mouse

was placed again into the white compartment. After 5 s, the door was raised. The step-through latency (STL-R) was recorded up to 300 s (Meunier et al., 2006, 2013; Villard et al., 2009, 2011). An exclusion criteria was STL-Tg and STL-R < 10 s. Animals showing these readouts are excluded from the calculations. Attrition is routinely < 5% in this test.

Object recognition test

Mice were placed individually in a squared open field. In session 1, animals acclimated for 10 min. In session 2, after 24 h, two identical objects were placed at ¼ and ¾ of one diagonal of the 50 x 50 cm^2 arena. The mouse activity and nose position were recorded during 10 min (Nosetrack® software, Viewpoint, Lissieu, France). The number of contacts with the objects and duration of contacts were measured. In session 3, after 1 h, the object in position 2 was replaced by a novel one differing in color, shape and texture. Each mouse activity was recorded during 10 min and analyzed. A preferential exploration index was calculated as the ratio of the number (or duration) of contacts with the object in position 2 over the total number (or duration) of contacts with the two objects. Animals showing no contact with one object or less than 10 contacts with objects, during the session 2 or 3, were discarded from the study. Attrition was 9% in this study.

Place learning in the water-maze

The water-maze was a circular pool (diameter 140 cm) and the platform (diameter 10 cm) was immersed under the water surface during acquisition. Swimming could be recorded using Videotrack® software (Viewpoint), with trajectories being analyzed as latencies and distances. Training consisted in 3 swims per day for 5 days. Start positions, set at each limit between quadrants, were randomly selected and each animal was allowed a 90 s swim to find the platform. Animals were left on the platform during 20 s. Animals that did not find the platform after 90 s had elapsed were placed on it manually and left for 20 s. Median latency was calculated for each training day and expressed as mean ± SEM. A retention probe test was performed 72 h after the last training without platform. The platform was removed, and each

animal was allowed a free 60 s swim. The 60-s duration swimming was videotracked and time spent in the training (T) quadrant analyzed *vs*. the averaged time spent in the 3 others (o). Animals did not receive drug treatment before the training sessions or probe test.

Topographic memory in the Hamlet test

The Hamlet (diameter 1.2 m) was elaborated by Viewpoint. It has a single level, 50 cm above the floor, with an agora at its center and streets expanding in a star shape towards five functionalized compartments, called houses. The walls and walkways are made of IR-transparent PVC. The room was uniformly illuminated (200 Lux). Infra-red emitting diodes are placed under the floor and an IR sensitive camera captures the animals' behaviors. The agora served as a gathering area and as a start box for training and test trials. The functionalized houses contained pellets (physiological function encoded: Eat), water (Drink), a novomaze (Viewpoint) (Hide), a running wheel (Run) or a grid isolating a stranger mouse (Interact).

Procedures and protocols have been previously described in detail (Crouzier et al., 2018; Crouzier and Maurice, 2018). In brief, animals were placed in the Hamlet in groups (all animals from the same housing cage) for 4 h per day during the 2-weeks training periods (Suppl. Fig. 1b). Two groups of animals were run in parallel, with one placed in the Hamlet between 8:00 am and 12:00 pm and the second between 12:30 pm and 4:30 pm. The topographic memory was evaluated in a probe test (PT0) after water-deprivation (WD) and compared to performance of the same animals in non-water deprived condition (NWD). 72 h after the last training session, WD consisted in removing the drinking bottle from the housing cage, 15 h before the probe test. WD or NWD animals were then placed individually in the agora and free to explore the Hamlet during a 10-min session. The exploratory behavior was videotracked and analyzed in terms of latency to reach the goal house and number of errors (entries into a street not directing to the goal house). $A\beta_{25-35}$ peptide was then injected ICV 2 h after the probe test (PT0) and the different drug treatments IP, and the probe test was reiterated after 7 days (PT7). A disorientation index (DI) was calculated for each variable (latency, errors) as the ratio between the mouse memory performance after and before $A\beta_{25-}$

$_{35}$ peptide treatment and subtracting the same values for control (V+V)-treated mice (Crouzier et al., 2018). No exclusion criterion was set.

Supplementary Figures

Supplementary Figure 1. Experimental protocols for anti-amnesia (**a**, **b**) and neuroprotection (**c**) experiments. Abbreviations: YMT, Y-maze test; PAT, step-through passive avoidance; ORT, object recognition test; WMT, water-maze test; †, sacrifice.

Supplementary Figure 2. Protective effects of Memantine and FENM, administered at 0.3 mg/kg IP, on the astroglial and microglial reactions in the cortex of $A\beta_{25-35}$-treated mice using (**a-e**) GFAP and (**f-j**) Iba-1 immunolabeling (**a-d, f-i**) typical immunofluorescence micrographs (Blue: DAPI, Green: GFAP, Red: Iba-1) and (**e, j**) quantifications. Coronal 25 µm thick sections were stained with anti-GFAP or anti-Iba-1 antibody and an area of the lateral parietal associative cortex analyzed as shown in Figure 6g. Scale in (a) = 50 µm. ANOVA: $F_{(3,22)}$ = 3.71, $p < 0.05$, in (e); $F_{(3,23)}$ = 6.43, $p < 0.01$, in (j). * $p < 0.05$, ** $p < 0.01$ *vs*. the (V+V)-treated group; ## $p < 0.01$ *vs*. the ($A\beta_{25-35}$+V)-treated group; Dunnett's test.

Suppl Figure 1

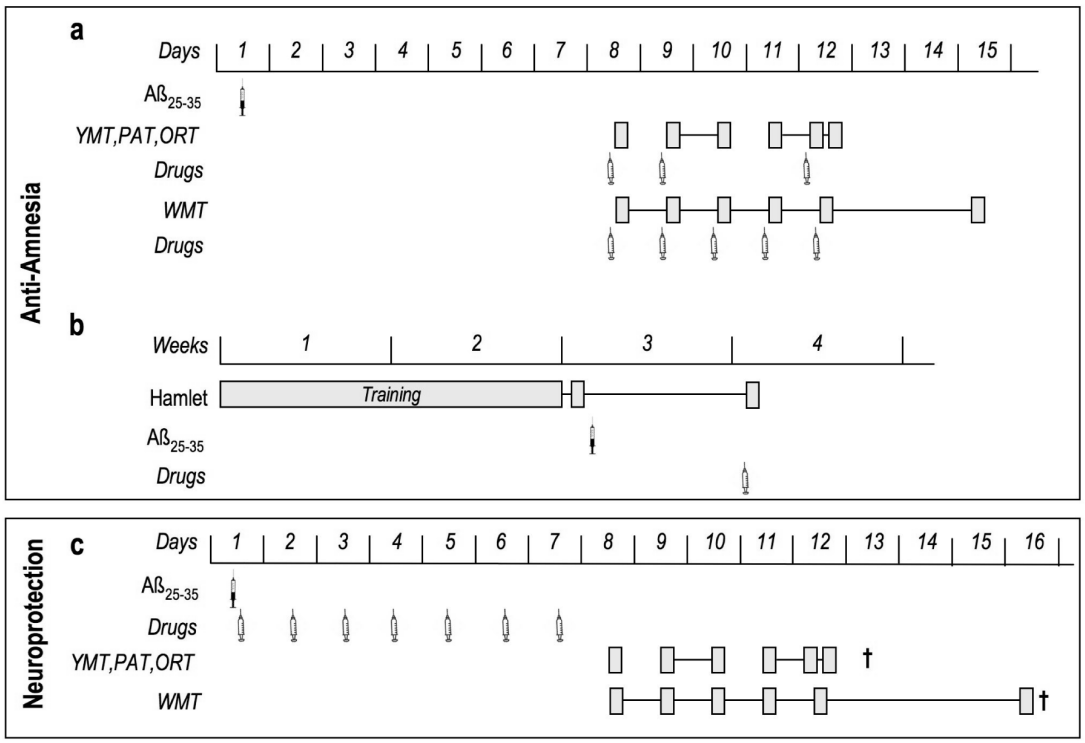

Suppl Figure 2